

SYNTHESIS OF ZEOLITES AND THEIR APPLICATIONS TO REMOVAL OF ARSENIC AND AMMONIA–NITROGEN FROM SAMPLES OF CONTAMINATED WATER

by

LINUS KWEKU LABIK, BSc(Hons)

**A Thesis Submitted to the School of Graduate Studies,
Kwame Nkrumah University of Science and Technology, Kumasi,
in partial fulfillment of the requirements for the degree
of**



**MASTER OF SCIENCE IN
MATERIALS SCIENCE**

College of Science

MAY, 2012

Abstract

The removal performance of arsenic and ammonia were investigated by adsorption process on Linde Type X (LTX), Low-Silica Type X and Linde Type A (LTA) zeolites. The zeolites were hydrothermally synthesized in the laboratory at $100^{\circ}\text{C} \pm 1^{\circ}\text{C}$. The synthesized zeolites were characterized by X-ray diffraction (XRD), Scanning electron microscopy (SEM), Fourier-Transformed Infra-red spectroscopy and Thermogravimetric analysis (TGA). The removal capacity of arsenic, known to be a hazardous contaminant in drinking water that causes arsenical dermatitis and skin cancer, and ammonia, which can have deleterious effects in water sources, were evaluated by adding 1.5 g and 0.8 g of zeolites to 100 ml and 50 ml of wastewater respectively for arsenic and ammonia removal. Removal efficiencies for Arsenic removal after treating for 30 minutes with adsorbents ranged between 67.86–81.35 % for LTX, 67.86–86.31 % for LSX and 71.87–96.00 % for LTA while removal efficiency of LTA for ammonia removal also ranged between 76.67–93.33 % and 86.15–90.77 % for treatment for 30 minutes (sample 1) and 60 minutes (sample 2) respectively. Langmuir and Freundlich isotherms were used in analysing results obtained from experimental studies. It was concluded that zeolites were efficient in removing arsenic and ammonia from contaminated water samples. The concentrations of arsenic and ammonia obtained after treatment were below the minimum contaminant levels as stipulated by the Ghana EPA. It is suggested that alternate methods like column and bed methods should be utilized to increase removal efficiencies and the use of local raw materials to synthesise the zeolites.

Dedication

This work is dedicated to my dad, Joseph Y. Labik, my family and friends.

KNUST



Contents

Declaration	i
Abstract	ii
Dedication	iii
List of Tables	x
List of Figures	xii
Acknowledgements	xiii
1 INTRODUCTION	1
1.1 Arsenic Contamination of Water Sources	1
1.1.1 Arsenic	1
1.1.2 Sources and Causes of Arsenic Contamination	2
1.1.3 Effects of Arsenic Contamination	2
1.2 Ammonia Contamination of Water Sources	3
1.2.1 Ammonia	3
1.2.2 Sources and Causes of Ammonia Contamination	3
1.2.3 Effects of Ammonia Contamination	3
1.3 Zeolites	3
1.4 Background to Study	5
1.5 Statement of Problem	6

1.6	Objectives	7
1.7	Justification	7
1.8	Importance	7
2	LITERATURE REVIEW	9
2.1	Zeolites	9
2.1.1	Historical Background	9
2.1.2	Zeolites and Zeolitic Materials	11
2.1.2.1	Molecular Sieves	11
2.1.2.2	Microporous and Mesoporous Materials	11
2.1.3	Zeolite Classification	12
2.1.4	Nomenclature of Zeolites	12
2.1.5	Structural Aspect	13
2.1.5.1	Channels and Pore Openings	14
2.1.6	Applications of Zeolites	15
2.1.6.1	Ion Exchange	15
2.1.6.2	Catalysis	15
2.1.6.3	Adsorption	16
2.1.6.4	Advanced Solid State Materials	16
2.1.6.5	Fillers	16
2.1.7	Diffusion in Zeolites	17
2.2	Structures Studied in this Work	18
2.2.1	Linde Type X (LTX)	18
2.2.2	Low Silica Type X (LSX)	19
2.2.3	Linde Type A (LTA)	19
2.3	Waste Water Samples	20
3	ION EXCHANGE PHENOMENA IN ZEOLITES	22

3.1	Ion Exchange Process	22
3.1.1	Adsorbent Capacity	22
3.1.2	Selectivity	22
3.1.3	Kinetics	23
3.2	Reactions and Equations	23
4	METHODOLOGY AND EXPERIMENTAL STUDIES	25
4.1	Introduction	25
4.2	Reagents and Apparatus	25
4.3	Synthesis of Zeolites	26
4.3.1	Linde Type X (LTX)	26
4.3.2	Low Silica Type X (LSX)	27
4.3.3	Linde Type A (LTA)	27
4.4	Characterization of Zeolites	28
4.4.1	X-ray Diffraction (XRD)	28
4.4.1.1	Introduction	28
4.4.1.2	Principle of XRD	28
4.4.1.3	Experimental method	29
4.4.2	Scanning Electron Microscopy (SEM)	30
4.4.2.1	Introduction	30
4.4.2.2	Principle of SEM	30
4.4.2.3	Experimental method	30
4.4.3	Fourier Transformed Infrared Analysis (FTIR)	30
4.4.3.1	Introduction	30
4.4.3.2	Principle of FTIR	30
4.4.3.3	Experimental method	31
4.5	Analysis of Arsenic in water samples	32

4.5.1	ICP–OES Analysis	32
4.5.1.1	Introduction	32
4.5.1.2	Principle of ICP-OES	32
4.5.1.3	Experimental method	33
4.6	Analysis of Ammonia in water samples	33
4.6.1	Photometer	33
4.6.1.1	Introduction	33
4.6.1.2	Principle of Photometer	33
4.6.1.3	Experimental method	34
4.7	Kinetic Studies	35
4.7.1	Wastewater Sampling	35
4.7.2	Batch Technique	35
4.8	Sorption Isotherms	36
4.8.1	Langmuir Isotherm	36
4.8.2	Freundlich Isotherm	37
5	RESULTS AND DISCUSSIONS	38
5.1	Synthesis and characterisation of Linde Type X	38
5.1.1	Synthesis	38
5.1.2	Characterisation	38
5.2	Synthesis and characterisation of Low Silica Type X	40
5.2.1	Synthesis	40
5.2.2	Characterisation	40
5.3	Synthesis and characterisation of Linde Type A	42
5.3.1	Synthesis	42
5.3.2	Characterisation	42
5.4	Analysis of Arsenic removal from samples by Zeolites	44

5.4.1	Kinetics	44
5.4.2	Sample 1 - NYAM 1	45
5.4.3	Sample 2 - NYAM 2	45
5.4.4	Sample 3 - NYAM 3	46
5.4.5	Sample 4 - NYAM 4	46
5.4.6	Sample 5 - NYAM 5	47
5.5	Analysis of Ammonia removal from samples using LTA	47
5.5.1	Sample 1	47
5.5.2	Sample 2	49
5.6	Sorption Isotherms	50
5.6.1	Linde Type X (LTX)	50
5.6.2	Low Silica Type X	51
5.6.3	Linde Type A	51
5.6.4	Langmuir and Freundlich Isotherms	53
5.7	Discussion	54
5.7.1	Zeolites	54
5.7.2	Arsenic Removal	55
5.7.3	Ammonia Removal	56
5.7.4	Other Variables Affecting Cation Exchange in Zeolites	56
6	CONCLUSION AND SUGGESTIONS FOR FUTURE WORK	58
6.1	Conclusion	58
6.2	Suggestions for future work	59
	Bibliography	61
A		68
A.0.1	Calculation to produce 0.01N NaOH	68

B.1 Used Softwares 72

KNUST



List of Tables

2.1	Difference between Zeolites and Molecular Sieves	11
5.1	General Infrared Assignments	40
5.2	Kinetics of Optimum Treatment Time	45
5.3	Results of Treatment of Sample 1 for Arsenic Removal	45
5.4	Results of Treatment of Sample 2 for Arsenic Removal	46
5.5	Results of Treatment of Sample 3 for Arsenic Removal	46
5.6	Results of Treatment of Sample 4 for Arsenic Removal	46
5.7	Results of Treatment of Sample 5 for Arsenic Removal	47
5.8	Results of Treatment 1 of Sample 1 for Ammonia Removal	48
5.9	Results of Treatment 2 of Sample 1 for Ammonia Removal	48
5.10	Results of Treatment 3 of Sample 1 for Ammonia Removal	48
5.11	Results of Treatment 4 of Sample 1 for Ammonia Removal	48
5.12	Results of 1st sample of Sample 2 for Ammonia Removal	49
5.13	Results of 2nd sample of Sample 2 for Ammonia Removal	49
5.14	Results of 3rd sample of Sample 2 for Ammonia Removal	49
5.15	Results of 4th sample of Sample 2 for Ammonia Removal	50
5.16	Langmuir parameters for adsorption of Arsenic	53
5.17	Freundlich parameters for adsorption of Arsenic	53
5.18	Langmuir parameters for adsorption of Ammonia	53
5.19	Freundlich parameters for adsorption of Ammonia	54

List of Figures

2.1	Tetrahedra framework structure of zeolites (www.bza.org/zeolites.html)	14
2.2	Framework structure of Linde Type X showing location of exchangeable sites (Kwakyee-Awuah, 2008)	19
2.3	(a) Channel system, (b) cages in LTA (Kulprathipanja, 2010)	20
2.4	Cation sites in LTA: (Kulprathipanja, 2010)	20
4.1	Schematic of the X-Ray Diffraction Spectrometer	29
4.2	Schematic of the FTIR Spectrometer	31
4.3	Schematic of the ICP-OES	32
5.1	SEM Micrographs of LTX	38
5.2	XRD of Linde Type X	39
5.3	FTIR Spectra of LTX	39
5.4	SEM Micrographs of Low-Silica Type X.	41
5.5	XRD Diffraction Patterns of LSX	41
5.6	FTIR Spectra of LSX	42
5.7	SEM micrographs of Linde Type A.	43
5.8	Diffraction Pattern of LTA	43
5.9	FTIR Spectra of LTA	44
5.10	(a) Langmuir isotherm model and (b) Freundlich isotherm model of LTX.	51
5.11	(a) Langmuir isotherm model and (b) Freundlich isotherm model of LSX.	51
5.12	(a) Langmuir isotherm model and (b) Freundlich isotherm model of LTA.	52

5.13 (a) Langmuir isotherm model and (b) Freundlich isotherm model of LTA for Ammonia treatment for 30 minutes.	52
5.14 (a) Langmuir isotherm model and (b) Freundlich isotherm model of LTA for Ammonia treatment for 60 minutes.	53
A.1 Thermogravimetric Analysis of LTX	69
A.2 Thermogravimetric analysis of LSX	69
A.3 Thermogravimetric Analysis of LTA	70
A.4 Results of ICP-OES from SGS Lab of Kinetics	70
A.5 Results of ICP-OES from SGS Lab of other Sample sites	71



Acknowledgments

I give thanks to God Almighty for His many blessings especially during the period of this work. To Him be glory and honour!

I am very grateful to my supervisor and lecturer, Dr. Bright Kwakye–Awuah for his guidance and corrections during this work. I am also grateful to the Head of Department, Prof. S. K. Danuor and all lecturers for their contributions to this work, may God richly bless you.

My appreciation goes to Dr. Boamah and the staff of the Civil Engineering, Water Research Group Lab for their help and support.

To Prof. Craig Williams for his help and contributions during the characterisation of the zeolites, I say “thank you”.

To my family and friends for their support and my dad especially for his contributions financially and encouragement, God bless you abundantly. Many thanks to my predecessors, Lizzy and Fred, for your advice and help. My colleagues at the Physics Department, it was great working with you.

To all who in many diverse ways have contributed in their own way, I couldn't have gotten to this point without your contributions, God bless you!

CHAPTER 1

INTRODUCTION

1.1 Arsenic Contamination of Water Sources

1.1.1 Arsenic

Arsenic occurs in many minerals, usually in conjunction with sulphur and other metals, and also as a pure elemental crystal or allotropes. Arsenic is a chemical element with the symbol As, atomic number 33 and relative atomic mass 74.92. In groundwater, arsenic combines with oxygen to form inorganic pentavalent arsenate and trivalent arsenite. Unlike other heavy metalloids and oxyanion-forming elements, arsenic can be mobilized under a wide range of oxidizing and reducing conditions at the pH values typically found in groundwaters (pH 6.5-8.5). Whereas all other oxyanion-forming elements are found within the $\mu\text{g/l}$ range, arsenic can be found within the mg/l range (Vu et al., 2003). Arsenic has four main chemical forms having oxidation states, -3, 0, +3, and +5, but in natural water its predominant forms are inorganic oxyanions of trivalent arsenite (As^{+3}) or pentavalent arsenate (As^{+5}) (Vu et al., 2003). The toxicity of different arsenic species varies in the order arsenite > arsenate > monomethylarsonate > dimethylarsinate. Trivalent arsenic is about 60 times more toxic than arsenic in the oxidized pentavalent state, and inorganic arsenic compounds are about 100 times more toxic than organic arsenic compounds (Vu et al., 2003). The organic forms of arsenic are found mostly in surface waters or in areas severely affected by industrial pollution. The relative concentrations of As(III) to As(V) vary widely, depending on the redox conditions in the geological environment (Vu et al., 2003).

Anthropogenic sources of arsenic may result from processing of a variety of ores (e.g., copper, gold, nickel, lead and zinc), from wool and cotton processing, from ingredients of many insecticides and herbicides, from additives to various metal alloys, from mining, from hazardous waste sites, or from

the glass and semi-conductor industry (Duarte et al., 2009). In general, groundwaters exhibit higher concentrations of arsenic species that are more toxic than those found in surface waters. It has been found that when river water – a primary source of drinking water – is polluted by industrial or mining effluents, or by geothermal waste, the arsenic concentration increases (Duarte et al., 2009).

1.1.2 Sources and Causes of Arsenic Contamination

Several industrial wastewater streams may contain heavy metals including the waste liquids generated by metal finishing or the mineral processing industries (Matis et al., 1998; Hui et al., 2005). The toxic metals, probably existing high concentrations (even up to 500 mg/l), must be effectively treated/removed from wastewaters, if the wastewaters are discharged directly into natural waters, it will constitute a great risk for the aquatic ecosystem (Matis et al., 2004). Their presence in streams and lakes has been responsible for the several types of health problems in animals and human beings (Bell, 2001). In Ghana, many communities depend on rivers for their economic and social activities.

1.1.3 Effects of Arsenic Contamination

All over the world industry is forced to diminish down to acceptable level contents of heavy metal in water and industrial wastewaters (Dąbrowski et al., 2004). The contamination of some water bodies through mining activities has been a major source of worry to industry, environmentalists, governments and other stakeholders for a very long time. The World Health Organisation has set the minimum contaminant level for Arsenic as 0.01 mg/l while that of the Ghana Environmental Protection Agency is 0.1 mg/l for drinking water. The presence of arsenic in rivers is responsible for the causes of skin cancer and other related skin problems such as arsenical dermatitis. Other effects include enlargement of the liver, heart diseases, internal cancers and neurological effects (Pontius, 1994). Over 300,000 people die of arsenic related diseases worldwide every year (Pontius, 1994).

1.2 Ammonia Contamination of Water Sources

1.2.1 Ammonia

Ammonia or azane is a compound of nitrogen and hydrogen with the formula NH_3 . It is a colourless gas with a characteristic pungent odor. Ammonia contributes significantly to the nutritional needs of terrestrial organisms by serving as a precursor to food and fertilizers. Ammonia, either directly or indirectly, is also a building-block for the synthesis of many pharmaceuticals and is used in many commercial cleaning products. Although in wide use, ammonia is both caustic and hazardous.

1.2.2 Sources and Causes of Ammonia Contamination

The WHO (1996) states that natural levels in groundwaters are usually below 0.2 mg/l of ammonia. Higher natural contents (up to 3 mg/l) are found in strata rich in humic substances or iron or in forests. Surface waters may contain up to 12 mg/l. Ammonia may be present in drinking-water as a result of disinfection with chloramines. Ammonia nitrogen discharges from municipal, industrial and agricultural wastewater sites which subsequently mixes into water resources (Rahmani et al., 2004)

1.2.3 Effects of Ammonia Contamination

Ammonia has a toxic effect on healthy humans only if the intake becomes higher than the capacity to detoxify (WHO, 1996). Some of the deleterious effects include accelerated eutrophication of lakes, dissolved oxygen depletion in receiving waters and fish toxicity (Rahmani et al., 2004; Nguyen and Tanner, 1998; Mercer et al., 1970).

1.3 Zeolites

Zeolites are crystalline aluminosilicates of group IA and group IIA elements, such as sodium, potassium, magnesium and calcium (Breck, 1974). The IUPAC defines zeolites as a subset of microporous or mesoporous materials containing voids arranged in an ordered manner and with a free volume larger than a 0.25 nm diameter sphere (McCusker et al., 2003). The Structure Commission of the International Zeolite Association uses the criterion of framework density (T-atoms per 1000 \AA^3) with the maximum

framework density for zeolites ranging from 19 to 21. Chemically, they are represented by the empirical formula:



where y is 2-200, n is the cation valence and w represents the water contained in the voids of the zeolite. Structurally, zeolites are complex, crystalline inorganic polymers based on an infinitely extending three-dimensional, four-connected framework of AlO_4 and SiO_4 tetrahedra linked to each other by the sharing of charges which is balanced by an extra-framework cation. The framework structure contains intracrystalline channels or interconnected voids that are occupied by the cations and water molecules. The cations are mobile and ordinarily undergo ion exchange. The water may be removed reversibly, generally by the application of heat, which leaves intact a crystalline host structure permeated by the micropores and voids which may amount to 50 % of the crystals by volume. The intracrystalline channels or voids can be one-, two- or three-dimensional. The preferred type has two or three dimensions to facilitate intracrystalline diffusion in adsorption and catalytic applications. More than 70 novel, distinct framework structures of zeolites are known (Kulprathipanja, 2010). They exhibit pore sizes from 0.3 to 1.0 nm and pore volumes from about 0.10 to 0.35 cm³/g. Typical zeolite pore sizes include: (i) small pore zeolites with eight-ring pores, free diameters of 0.30–0.45 nm (e.g., zeolite A), (ii) medium pore zeolites with 10-ring pores, 0.45–0.60 nm in free diameter (ZSM-5), (iii) large pore zeolites with 12-ring pores of 0.6–0.8 nm (e.g., zeolites X, Y) and (iv) extra-large pore zeolites with 14- ring pores (e.g., UTD-1). The zeolite framework should be viewed as somewhat flexible, with the size and shape of the framework and pore responding to changes in temperature and guest species. For example, ZSM-5 with sorbed neopentane has a near-circular pore of 0.62 nm, but with substituted aromatics as the guest species the pore assumes an elliptical shape, 0.45 to 0.70 nm in diameter. Some of the more important zeolite types, most of which have been used in commercial applications, include the zeolite minerals mordenite, chabazite, erionite and clinoptilolite, the synthetic zeolite types A, X, Y, L, “Zeolon” mordenite, ZSM-5, beta and MCM-22 and the zeolites F and W. In this work, Linde Type X, Low-Silica type X and Linde Type A are used.

1.4 Background to Study

Waste water treatment has been wide spread due to new and stringent measures to reduce the amount of pollution caused by industrial companies especially the mining sector. Many methods are currently under research including the use of zeolites to treat the waste water before they are released into the environment i.e. water bodies. Several treatment technologies have been adopted to remove arsenic and ammonia from drinking water under both laboratory and field conditions. The major modes of removing arsenic from water is by physical - chemical treatment. Most conventional treatments fall into four process categories: ion exchange, membrane process, adsorption and chemical precipitation. Ion-exchange treatments are very limited in their ability to remove arsenic depending on exchange competition from other anions. Membrane processes are very effective at removing arsenic from groundwater, but the cost is high. Accordingly, adsorption and chemical precipitation processes are being explored for low-cost, effective treatments (Vu et al., 2003).

Rahmani and Mahvi (2006) have stated that the three most widely used methods for removal of ammonium from polluted water are air stripping, ion exchange and biological nitrification. Zeolites have been used as adsorbents, molecular sieves, membranes, ion exchanger and catalysts in municipal and industrial pollution control, as well as in horticulture, agriculture, and environmental soil remediation – but their primary use has been in water and wastewater treatment (Meteš et al., 2004). The chemical and structural features of zeolites make them very effective for the removal of toxic metal ions (Meteš et al., 2004). Conventional methods like precipitation are unfavourable especially when dealing with large volumes of matter which contains heavy metals in low concentration (Dąbrowski et al., 2004). Zeolites have a three-dimensional structure constituted by $(\text{Si}, \text{Al})\text{O}_4$ tetrahedra connected by all their oxygen vertices forming channels where H_2O molecules and exchangeable cations counterbalance the negative charge generated from the isomorphous substitution. Synthetic zeolites are useful because of their controlled and known physico-chemical properties (Shevade and Ford, 2004). The focus of this project is to study the efficacy of the zeolites: Linde Type X, Low-Silica Type X and Linde Type A in removing Arsenic from the River Nyam in Obuasi and ammonia from wastewater collected from the

KNUST Waste treatment plant. The use of zeolite for wastewater treatment has been carried out in many countries.

1.5 Statement of Problem

Water is life! This simple statement embodies the importance of water to individuals, families, communities, nations and regions. Without adequate water, the human body does not survive and when droughts occur, they create famine to destroy prosperous societies. All over the World, civilisation occurred around water bodies and the banks of ancient rivers such as the Tigris and Euphrates, the Nile, the Niger, Zambezi and many more had been the pivot of growth and great Civilisations and in Ghana, many communities derive their names from rivers e.g. Praso, Nyamso, Offinso, Tanoso. Water provides an environment for healthy populations, serves the aesthetic and spiritual needs of societies and also forms the basis of agriculture and industries. Sustainable socio-economic progress is seldom possible without adequate development of water resources to support food production, industry, the environment and other human needs. Indigenous communities place high value on land and water bodies because most traditional societies depend on land-based economic activities for their livelihoods. The River Nyam is the closest river to the AngloGold Ashanti Mine operations in the Obuasi Municipality and runs through some communities. The people of Nyamso and surrounding communities depend on the River Nyam for their fishing and farming activities and also for domestic use in cooking, washing and cleaning. The presence of arsenic in water supplies has been linked to arsenical dermatitis, skin cancer, neurological effects, enlargement of liver, heart disease and internal cancers (Shevade and Ford, 2004; Pontius, 1994; Hui et al., 2005).

Ammonia nitrogen discharged into water resources from municipal, industrial and agricultural wastewater sites also contributes to the pollution of water bodies through and not limited to accelerated eutrophication, dissolved oxygen depletion in receiving waters and fish toxicity (Rahmani and Mahvi, 2006; Rahmani et al., 2004). The need to treat contaminated water bodies is very urgent due to the dependence of many farmers for their activities and also due to the increasing demand for potable water supply in our urban and rural areas.

1.6 Objectives

The aim of this project is to investigate the efficiency of synthetic zeolite in removing some contaminants from fresh water bodies hence making the water safe for consumption and contribute to the reduction of water pollution. The specific objectives include:

1. To synthesize and characterize different types of zeolites (i.e. Linde Type X, Low-Silica Type X and Linde Type A).
2. To characterize the phase purity, thermal, vibrational, morphological and elemental composition of the synthesized zeolites.
3. To investigate the efficiency of the synthesized zeolites in removing the contaminants.

1.7 Justification

The use of zeolites in waste water treatment and their applications to removing harmful pollutants is well documented. In addition, zeolites are also used as antimicrobial agents in some developed countries. Zeolites are extensively used in industries as ion exchangers and catalysts in a large range of processes. Diffusion of ions in zeolites differs greatly from diffusion in liquids and gases due to the presence of pores that makes their framework. These framework structures of zeolites determine the ease or speed with which substances enter or leave the active centers. Not much research has been done on the use of zeolites in waste water treatment in Sub-Saharan Africa, thus, this project will provide knowledge on the efficacy of zeolites in removing arsenic and ammonia from some water samples.

1.8 Importance

The importance of zeolites in various industries cannot be understated. The work proposed in this study will be the first of its kind in the country. The results will benefit the health sector, water treatment agencies, industries as most of the toxic compounds will be removed from effluents before they are released into river bodies. It will also be a basis for extended research into the use of local materials in

the synthesis of zeolites for local use especially in the mining industry and also for water treatment for local consumption in areas with polluted waters due to industrial activities. Thus, increase availability of potable water to both rural and urban dwellers.

KNUST



CHAPTER 2

LITERATURE REVIEW

2.1 Zeolites

2.1.1 Historical Background

The history of zeolites began in 1756 when the Swedish mineralogist Cronstedt discovered the first zeolite mineral, stilbite in Cronstedt (1756) as cited in Kulprathipanja (2010). The word Zeolite is from two greek words zein meaning “boiling” and lithos meaning “stone” (Szostak, 1989; Breck, 1974; Kwakye-Awuah, 2008).

As cited y Kwakye-Awuah (2008) zeolites are found to be characterised by the following properties:

- Catalytic properties;
- High hydration propensity;
- Stable crystal structure when dehydrated;
- Low density and high void volume when dehydrated;
- Cation exchange and sorption properties.

As cited in Kulprathipanja (2010), various authors have described the properties of zeolite minerals, including adsorption properties and reversible cation exchange and dehydration, i.e. St. Claire Deville reported the first hydrothermal synthesis of a zeolite, levynite, in 1862; In 1896 Friedel developed the idea that the structure of dehydrated zeolites consists of open spongy frameworks after observing that various liquids such as alcohol, benzene and chloroform were occluded by dehydrated zeolites;

Grandjean in 1909 observed that dehydrated chabazite adsorbs ammonia, air, hydrogen and other molecules and in 1925 Weigel and Steinhoff reported the first molecular sieve effect. They noted that dehydrated chabazite crystals rapidly adsorbed water, methyl alcohol, ethyl alcohol and formic acid but essentially excluded acetone, ether or benzene (Weigel and Steinhoff, 1925). The first use of X-ray diffraction for identification in mineral synthesis was reported by Leonard in 1927 (Leonard, 1927). Taylor and Pauling described the first single crystal structures of zeolite minerals in 1930 (Taylor, 1930; Pauling, 1930b;a). McBain in his book in 1932 established the term “molecular sieve” to define porous solid materials that act as sieves on a molecular scale (McBain, 1932). Thus, by the mid-1930s the literature described the ion exchange, adsorption, molecular sieving and structural properties of zeolite minerals as well as a number of reported syntheses of zeolites. In his pioneering work in zeolite adsorption and synthesis in the mid-1930s to 1940s R. M. Barrer presented the first classification of the then-known zeolites based on molecular size considerations in Barrer (1945) and reported the first definitive synthesis of zeolites, including the synthetic analog of the zeolite mineral mordenite (Barrer, 1948b) and a novel synthetic zeolite (Barrer, 1948c;a) much later identified as the KFI framework. Between 1949 and 1954 R. M. Milton and co-worker Donald W. Breck of the Linde Division of Union Carbide discovered a number of commercially significant zeolites, types A, X and Y. In 1954, Union Carbide commercialized synthetic zeolites as a new class of industrial materials for separation and purification. The earliest applications were the drying of refrigerant gas and natural gas. In 1955, T.B. Reed and D.W. Breck reported the structure of the synthetic zeolite A (Kulprathipanja, 2010). In 1959, Union Carbide marketed the “ISOSIV” process for normal-isoparaffin separation, representing the first major bulk separation process using true molecular sieving selectivity. Also in 1959, a zeolite Y-based catalyst was marketed by Carbide as an isomerization catalyst (Milton, 1989). Zeolites can be natural or synthetic with more than 150 zeolite types synthesized and 40 naturally occurring zeolites known as reported in Szostak (1989) and cited by Kwakye-Awuah (2008). Natural zeolites are formed from volcanic ash while synthetic zeolites are produced mainly in the laboratory.

2.1.2 Zeolites and Zeolitic Materials

2.1.2.1 Molecular Sieves

Molecular sieves are porous solids with pores of the size of molecular dimensions, 0.3-2.0 nm in diameter (Kulprathipanja, 2010). The term “molecular sieves” was introduced to describe those materials that exhibit selective adsorption properties (Szostak, 1989; Kwakye-Awuah, 2008). Examples include zeolites, carbons, glasses and oxides. Some are crystalline with a uniform pore size delineated by their crystal structure, for example, zeolites. Most molecular sieves in practice today are zeolites.

Table 2.1 Difference between Zeolites and Molecular Sieves

Zeolites	Molecular sieves
Special class of molecular sieves with aluminosilicates as skeletal composition	Composition varies and distinguishes materials on the basis of their size
They are highly crystalline materials	May be crystalline, non-crystalline, para-crystalline or pillared clays
Anionic framework with microporous and crystalline structure	Variable charged framework with porous structure

2.1.2.2 Microporous and Mesoporous Materials

Porous materials are classified into several kinds by their size. According to the IUPAC notation, microporous materials have pore diameters of less than 2 nm, mesoporous materials have pore diameters between 2 nm and 50 nm and macroporous materials have pore diameters of greater than 50 nm (Rouquerol et al., 1994). Microporous materials are often used in laboratory environments to facilitate contaminant-free exchange of gases. Mold spores, bacteria, and other airborne contaminants will become trapped, while allowing gases to pass through the material. This allows for a sterile environment in the contained area. Typical mesoporous materials include some kinds of silica and alumina that have similarly-sized fine mesopores. Mesoporous oxides of niobium, tantalum, titanium, zirconium, cerium and tin have also been reported. According to the IUPAC, a mesoporous material can be disordered or ordered in a mesostructure (Rouquerol et al., 1994). Notable examples of prospective applications of mesoporous materials are catalysis, sorption, gas sensing, ion exchange, optics, and photovoltaics.

2.1.3 Zeolite Classification

There are 3 groups based on the Al/Si ratio in the framework into which zeolites may be classified. Two of these are based upon specifically defined aspects of crystal structure, and the third has a more historical basis, placing zeolites with similar properties such as morphology into the same group (Barrer, 1982; Szostak, 1989). Zeolites can be classified by considering the topology of the framework without regard to chemical composition (for example, by considering a framework consisting of SiO_2 only) and choosing the highest possible symmetry for the topology. All zeolites having the same topology constitute a zeolite framework type. In using the basic building unit (BBU) or secondary building unit (SBU) model for zeolite classification, the basic building unit framework in a zeolite is a TO_4 tetrahedron where the central T-atom is typically Si or Al and the peripheral atoms are O. The third broad classification scheme is similar to the secondary building unit (SBU) classification of Breck (1974), except that it includes some historical context of how the zeolites were discovered and named. This scheme uses a combination of zeolite group names which have specific SBUs and is widely used by geologists. This is the classification scheme used by Ocelli and Kessler (1997) as stated by Kwakye-Awuah (2008).

2.1.4 Nomenclature of Zeolites

There is no systematic nomenclature developed for molecular sieve materials. The discoverer of a synthetic species based on a characteristic X-ray powder diffraction pattern and chemical composition typically assigns trivial symbols (Kulprathipanja, 2010). The early synthetic materials discovered by Milton, Breck and coworkers at Union Carbide used the modern Latin alphabet, for example, zeolites A, B, X, Y, L. The use of the Greek alphabet was initiated by Mobil and Union Carbide with the zeolites alpha, beta, omega. Many of the synthetic zeolites which have the structural topology of mineral zeolite species were assigned the name of the mineral, for example, synthetic mordenite, chabazite, erionite and offretite. The molecular sieve literature is replete with acronyms: ZSM-5, -11, ZK-4 (Mobil), EU-1, FU-1, NU-1 (ICI), LZ-210, AlPO, SAPO, MeAPO, etc. (Union Carbide, UOP) and ECR-1 (Exxon). The one publication on nomenclature by IUPAC in 1979 is limited to the then-known zeolite-type materials (Barrer, 1979). The Atlas of Zeolite Structure Types (Baerlocher et al., 2007), which is published and

frequently updated by the International Zeolite Association Structure Commission, assigns a three-letter code to be used for a known framework topology irrespective of composition, examples include LTA for Linde zeolite A, FAU for molecular sieves with a faujasite topology (e.g., zeolites X, Y), MOR for the mordenite topology, MFI for the ZSM-5 and silicalite topologies and AFI for the aluminophosphate AIPO4-5 topology. The IZA Structure Commission must approve a newly determined structure of a zeolite or molecular sieve before it is included in the official Atlas. The definition and usage of the term “zeolite” has evolved and changed, especially over the past decade, to include non-aluminosilicate compositions and structures. The inclusion of a structure in the Atlas is limited to three-dimensional, tetrahedral oxide networks with a framework density less than about 21 T-atoms per 1000 Å³ irrespective of framework composition. Similarly the term zeolite has been broadened in the mineralogy literature to include tetrahedral framework compositions with T-elements other than Al and Si but where classic zeolite properties are exhibited (e.g., structures containing open cavities in the form of channels and cages, reversible hydration–dehydration characteristics as cited in Kulprathipanja (2010)). Very recently as a sign of the times the term “nanoporous” materials has been applied to zeolites and related molecular sieves (Kulprathipanja, 2010). For this research, Linde Type X, Low Silica Type X and Linde Type A have been studied and will be assigned the letters LTX, LSX and LTA respectively.

2.1.5 Structural Aspect

Traditionally, zeolites are considered to be a subset of the molecular sieve family with structures based on an infinitely extending three-dimensional, four-connected framework of AlO₄ and SiO₄ tetrahedra linked to each other by the sharing of oxygen atoms. However, the usage of the term “zeolite” has evolved to include tetrahedral oxide structures with framework atoms other than Al and Si, but where zeolitic properties are exhibited (e.g., channels, voids, reversible hydration–dehydration). The framework structure of a zeolite defines intracrystalline voids and channels occupied by cations (to balance the net negative charge for each AlO₄ in the framework), water molecules and perhaps other guest species (Kulprathipanja, 2010). The balancing of charges in the frameworks creates the resulting high cation exchange capability reported in Occelli and Kessler(1997) and Ertl et al.(1999) and cited by

Kwakye-Awuah (2008). Exchangeable cations include lithium, cadmium, lead, zinc, copper, ammonia, silver and protons. There are hundreds of different possible three-dimensional lattice structures. The large majority of zeolites are constructed from Secondary Building Units (SBUs) which are component units with up to 16 T-atoms that are derived assuming that the entire framework is made up of only one type of unit only.

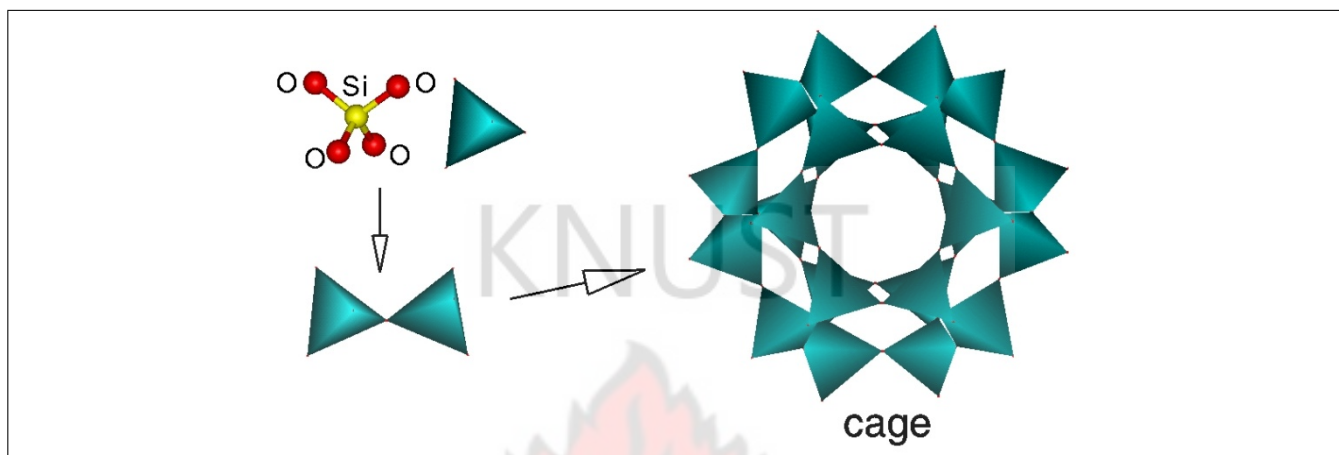


Figure 2.1: Tetrahedra framework structure of zeolites (www.bza.org/zeolites.html)

2.1.5.1 Channels and Pore Openings

Zeolite structures are often described according to the size of pore openings and the dimensionality of their channel system (Szostak, 1989). Kulprathipanja (2010) describes the n-rings (where n is the number of T atoms in the ring, where T = Al or Si tetrahedra) defining the face of a polyhedral composite building units (CBUs) (formed by combining several BBUs) as windows or pores and pores that are infinitely extended in one dimension and are large enough to allow diffusion of guest species (i.e., larger than six-rings) as channels. An important characteristic of zeolites is the effective width of the channels which determines the accessibility of the channels to guest species. The effective width is limited by the smallest free aperture along the channel (Kulprathipanja, 2010). Different pore openings are assigned for different ring sizes. Hence an 8-ring is considered a small ring opening, a 10-ring opening is considered a medium ring opening and a 12-ring is considered a large ring opening (Breck, 1974; Szostak, 1989).

The size and shape of the pore opening depends on:

1. The configuration of the T and O atoms relative to each other

2. The Si/Al ratio
3. The size of the cation
4. The location of the cation
5. Temperature (Szostak, 1989)

2.1.6 Applications of Zeolites

Zeolites have been in use for several decades and mostly in petroleum refining and in detergents as a replacement for phosphates (Kulprathipanja, 2010). However, the main applications of zeolites are adsorption, catalysis and ion exchange (Szostak, 1989). Applications of zeolites include the following.

2.1.6.1 Ion Exchange

The loosely-bound nature of extra-framework cations allows them to be readily exchanged for other types of cations including metal ions when they are in aqueous solution (Townsend, 1986; Kwakye-Awuah, 2008; Rahmani and Mahvi, 2006). The cation-exchange behaviour of zeolites depends on: the nature, size and charge of the cation species, temperature and the concentration of the cationic species in the solution, the anion associated with the cation in solution, the type of solvent and the structural characteristics of the particular zeolite (Szostak, 1989). Zeolite ion exchange products, both synthetic and natural, were used extensively in nuclear waste cleanup after the Three Mile Island and Chernobyl nuclear accidents. New applications emerged for zeolite powders in two potentially major areas, odor removal and as plastic additives (Kulprathipanja, 2010). The use of zeolites for removal of heavy metals and other water pollutants have also been reported (Zorpas et al., 2000; Shevade and Ford, 2004; Rahmani and Mahvi, 2006).

2.1.6.2 Catalysis

Zeolites are extremely useful as catalysts for several important reactions involving organic molecules (Szostak, 1989). The most important are cracking, isomerization and hydrocarbon synthesis. Zeolites are able to promote a diverse range of catalytic reactions including acid-base and metal induced reactions; serve as acid catalysts and can be used to support active metals or reagents as in Barthomeuf (1996) cited

by Kwakye-Awuah (2008). Sobolev et al.(1993) reported that zeolites can be shape-selective catalysts either by transition state selectivity or by exclusion of competing reactants on the basis of molecular diameter (Kwakye-Awuah, 2008). They have also been used as oxidation catalysts. The reactions can take place within the pores of the zeolite, which allows a greater degree of product control (Szostak, 1989). Zeolites are used as catalysts in the production of organic (fine) chemicals and in detergents as a replacement for phosphates (Kulprathipanja, 2010) and petroleum refining (Kwakye-Awuah, 2008).

2.1.6.3 Adsorption

Zeolites are used to adsorb a variety of materials. This includes applications in drying, purification and separation. Kulprathipanja (2010) reports that environmentally driven applications have arisen recently, causing the use of hydrophobic molecular sieves, highly siliceous Y zeolite and silicalite, for the removal and recovery of volatile organic compounds (VOCs). The porous structure of zeolites can be used to “sieve” molecules having certain dimensions and allow them to enter the pores (Kwakye-Awuah, 2008; Hui et al., 2005).

2.1.6.4 Advanced Solid State Materials

In a 1989 review, Ozin et al. (1989) speculated “that zeolites (molecular sieves) as microporous molecular electronic materials with nanometer dimension window, channel and cavity architecture represent a ‘new frontier’ of solid state chemistry with great opportunities for innovative research and development”. The applications described or envisioned included: molecular electronics, “quantum” dots/chains, zeolite electrodes, batteries, non-linear optical materials and chemical sensors. More recently there have been significant research reports on the use of zeolites as low k dielectric materials for microprocessors (Wang et al., 2001a;b). Zeolites have also been used as raw materials for ceramic compositions relevant to the electronic industry. Bedard et al. reported the high-temperature processing of zeolite B (P) to form cordierite ceramic compositions (Bedard et al., 1991).

2.1.6.5 Fillers

Zeolites are also used as fillers in the manufacture of papers (Kulprathipanja, 2010).

2.1.7 Diffusion in Zeolites

Kwakye-Awuah (2008) citing from Karger and Ruthven (1992) defines diffusion as a phenomenon of random motion causing a system to decay towards uniform conditions. Diffusion is caused by the thermal motion and subsequent collision of molecules in a closed system. Two types of diffusion can be distinguished: transport diffusion, which is initiated by a concentration gradient, and self-diffusion, which takes place in a system that is in equilibrium (Szostak, 1989; Kwakye-Awuah, 2008). Diffusion of molecules through the pores of zeolites is different from diffusion in fluids or large porous solids. Since the molecules have to move through channels of molecular dimensions there is a constant interaction between the zeolite framework and the diffusion molecules (Szostak, 1989). Hence the molecular motion is highly influenced by both the size and shape of the channels instead of temperature and concentration only cited in Kwakye-Awuah (2008). In Szostak (1989) the diffusivity in this region depends on:

- The pore diameter
- The structure of the pore wall
- The interaction between the surface atoms and the diffusion molecules
- The shape of the diffusion molecules and
- The way they are connected.

Diffusion in zeolites can be classified in a number of different regimes depending on the pore diameter. For large pore diameters of the order of $1\ \mu\text{m}$ or greater, usually called macropores, collisions between the molecules occur much more frequently than the collisions with the walls Thompson (1998) as cited by Kwakye-Awuah (2008). As the size of the pores decreases, the number of collisions with walls increases until it finally becomes smaller than the mean free path (the average distance travelled by a molecule between collisions). At this point Knudsen diffusion takes over and the mobility of the molecules start to depend on the dimensions of the pore (Szostak, 1989; Kwakye-Awuah, 2008). At smaller pore sizes

in the range of 20 Å the interaction between the molecules and the walls is constant. Diffusion in the micropores of zeolites takes place in this region and is called configurational diffusion by Thompson (1998) (Kwaky-Awuah, 2008).

2.2 Structures Studied in this Work

2.2.1 Linde Type X (LTX)

Linde Type X (Figure 2.2) is a synthetic counterpart of the naturally occurring mineral Faujasite (Breck, 1974; Szostak, 1989). It has one of the largest cavities and cavity entrances of any known zeolites (Szostak, 1989). The channel structure is 3-dimensional with equidimensional channels intersecting in a perpendicular order with free aperture of 7.4 Å which was reported in Coutinho and Balkus (2002) and cited by Kwaky-Awuah (2008). There are also smaller cavities called sodalite cages which are connected to the supercages by rings of four and six tetrahedra (Szostak, 1989). Exchangeable cations, which balance the negative charge of the aluminosilicate framework, are found within the zeolite cavities. They are usually found (Yeom and Kim, 1997) at the following sites shown in Figure 2.2: site I at the centre of a D6R, site I' in the sodalite cavity on the opposite side of one of the D6R's 6-rings from site I, II' inside the sodalite cavity near a single 6-ring entrance to the supercage, II in the supercage adjacent to a S6R, III in the supercage opposite a 4-ring between two 12-rings, and III' off III (off the 2-fold axis) (Szostak, 1989). The chemical composition can vary according to the silicon and aluminum content from a Si/Al ratio = 1.0-1.5. Zeolite X has a wide range of industrial application primarily due to the excellent stability of the crystal structure and a large available pore volume and surface area (Kwaky-Awuah et al., 2008; Kwaky-Awuah, 2008).

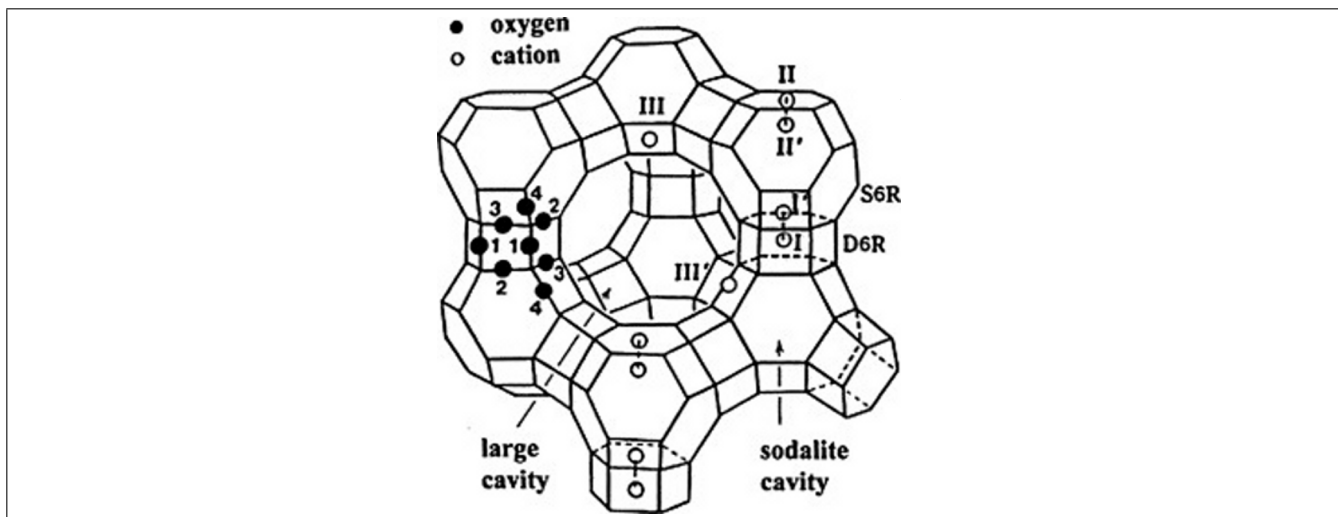


Figure 2.2: Framework structure of Linde Type X showing location of exchangeable sites (Kwakye-Awuah, 2008)

2.2.2 Low Silica Type X (LSX)

Zeolite LSX is in the faujasite (FAU) family with a framework containing double 6 rings linked through sodalite cages that generate supercages with pore diameters of 7.4 (Khemthong et al., 2007). The typical Si/Al ratio of LSX is in the range of 1 - 1.5. It belongs to the space group F_{3m} and has a large number of extra-framework cations. LSX can be synthesized from a variety of silica sources including natural clay such as kaolinite, oil shale ash, and commercial silicates (Khemthong et al., 2007). Thus, its structure is similar to that of Linde Type X.

2.2.3 Linde Type A (LTA)

The LTA (Linde Type A) structure (Figure 2.3) has a 3-dimensional pore structure with pores running perpendicular to each other in the x, y, and z planes, and is made of secondary building units 4, 6, 8, and 4-4 (Szostak, 1989). The pore diameter is defined by an eight member oxygen ring and is small at 4.2 Å leading to a larger cavity of minimum free diameter 11.4 Å (Kwakye-Awuah, 2008). The cavity is surrounded by eight sodalite cages (truncated octahedra) connected by their square faces in a cubic structure. The unit cell is cubic ($a = 24.61 \text{ \AA}$) with $Fm-3c$ symmetry. LTA has a void volume fraction of 0.47, with a Si/Al ratio of 1.0 (Szostak, 1989). It is stable at temperatures up to 700 °C at which it thermally decomposes (Kwakye-Awuah, 2008). Primary cation sites (Figure 2.4) are: site I (centered on the six-rings and displaced into the alpha cavity), site II (near the center of the eight-rings and close to

the eight-ring planes) and site III (centered on the four-rings and displaced into the alpha cavity). Sites I, II and III can accommodate 8, 3 and 12 cations per alpha cavity, respectively, and cations tend to prefer sites in the order I, then II, then III. Since site II is near the center of the eight-ring, cations which occupy site II will affect diffusion (Kulprathipanja, 2010).

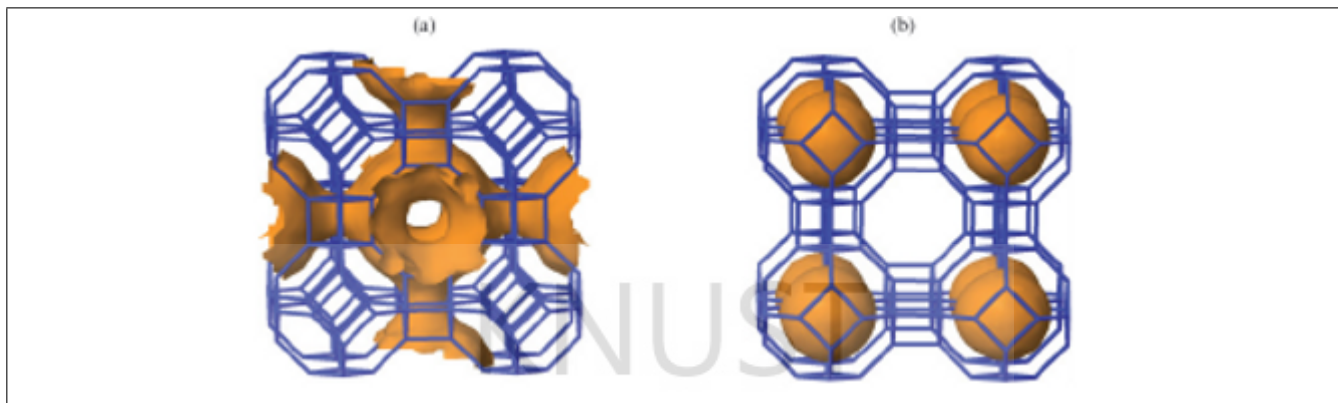


Figure 2.3: (a) Channel system, (b) cages in LTA (Kulprathipanja, 2010)

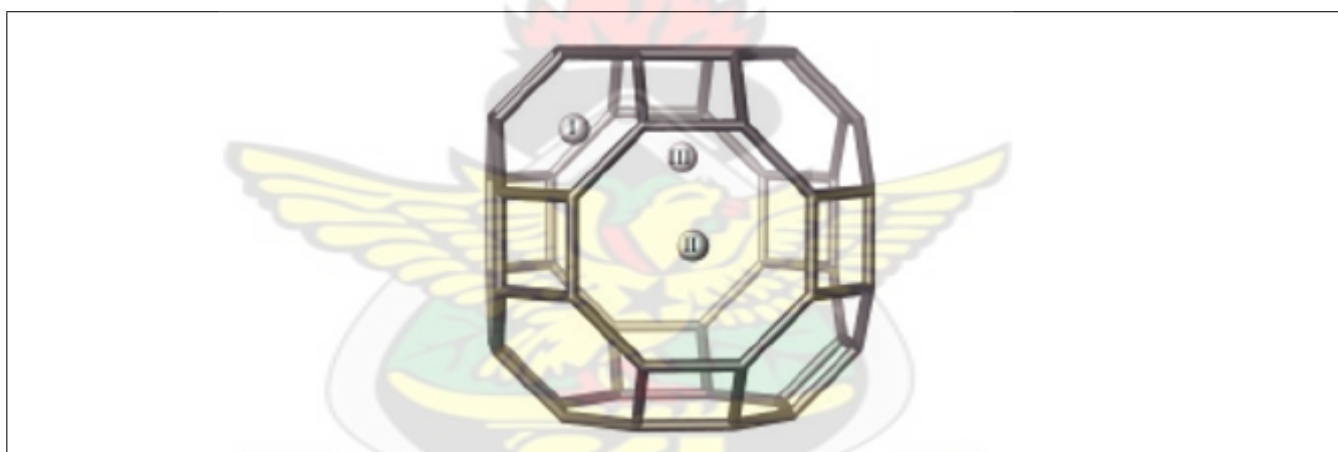


Figure 2.4: Cation sites in LTA: (Kulprathipanja, 2010)

2.3 Waste Water Samples

Initial waste water samples collected to check their contaminant levels included Rivers Jimi (Obuasi), River Nyam (Ouasi), River Birim (Kyebi) and River Wewe (KNUST, Kumasi). After initial measurements for contaminant levels, River Nyam which is very near the tailings disposal site of AngloGold Ashanti Company was chosen since it had the highest measured amount of Arsenic. The measured amount was above the maximum contaminant level set by the Ghana Environmental Protection Agency. Therefore water samples collected from the River Nyam were used in arsenic removal. Samples were taken monthly for 5 months. Nitric acid (HNO_3) as preservative was added to the collected water

samples to be used for arsenic analysis.

Two water samples were collected from the KNUST waste water Treatment Centre and preserved through refrigeration.

Methods of preservation are relatively limited and are intended generally to (1) retard biological action, (2) retard hydrolysis of chemical compounds and complexes, (3) reduce volatility of constituents, and (4) reduce absorption effects. Preservation methods are generally limited to pH control, chemical addition, refrigeration, and freezing (U.S.E.P.A, 1983).



CHAPTER 3

ION EXCHANGE PHENOMENA IN ZEOLITES

3.1 Ion Exchange Process

Zeolitic adsorbents are composed of a large number of ionic (or potentially ionic) sites. The framework contains channels and interconnected voids occupied by cations and water molecules. The cations are mobile and can be exchanged with other cations to varying degrees. In ion exchange separation, cations in liquid are reversibly exchanged with cations in a solid adsorbent. More specifically, cations are interchanged with other cations without changing the structure of zeolites. At equilibrium, electroneutrality in both zeolite and liquid phases is maintained. Liquid separation based on ion exchange is important in industrial applications. Critical factors to consider in developing an ion exchange separation process are adsorbent capacity, selectivity and kinetics (Kulprathipanja, 2010).

3.1.1 Adsorbent Capacity

Ion exchange capacity is a measure of the quantity of cations adsorbed or removed by the zeolitic adsorbent. The total capacity of a zeolite is a function of its $\text{SiO}_2/\text{Al}_2\text{O}_3$ mole ratio (Kulprathipanja, 2010). As stated in Kwakye-Awuah (2008), the cation exchange capacity (CEC) as defined by Ertl *et al.*, (1999) is the magnitude of cation exchange written as

$$CEC = \frac{\text{the number of cations available for exchange}}{\text{the sum of the atomic weights of constituent atoms}} = \frac{N_c}{A_m} \quad (3.1)$$

3.1.2 Selectivity

In general, zeolites have higher ion exchange selectivity for higher-charged cations. For cations having the same valence, the ion exchange selectivity often depends on the hydrated ionic radius. This is seen from the zeolite ion exchange selectivity decreasing with ionic radii (Kulprathipanja, 2010).

3.1.3 Kinetics

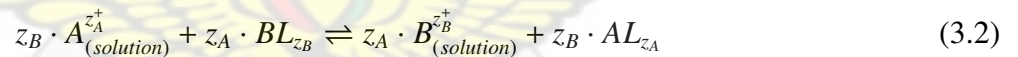
Ion exchange involves the formation and breakage of bonds between ions in solution and exchange sites in a zeolitic adsorbent. The reaction equilibrium of the ion exchange process depends most significantly on:

1. Contact time,
2. Operating temperature and
3. Ionic concentration.

KNUST

3.2 Reactions and Equations

Townsend (1986) states that there are two alternative and equally valid ways of expressing a binary exchange reaction (and consequently the thermodynamic equilibrium constant). The first of these (most commonly employed was used by Vanselow (1932):



where z_A and z_B are respectively the valencies of the exchanging cations A and B. There are of course present also in the external solution co-anions Y, which maintain electro-neutrality in that phase, and these co-anions may be regarded as providing the “exchange capacity” of the electrolyte solution external to the zeolite. L is defined as a portion of zeolite framework holding unit negative charge. He states a second way of expressing the reaction which is traced to Gapon (1933):



The stoichiometric quantities of A, B, L (and consequently Y) involved in equation 3.3 are seen to be the same as in equation 3.2, making equation 3.3 an alternative (if less familiar) way of express the exchange reaction.

From equation 3.2, the following (familiar) definition of the thermodynamic equilibrium constant

follows:

$$K_a = (a_{B,s}^{z_A} / a_{A,s}^{z_B}) (a_A^{z_B} / a_B^{z_A}) \quad (3.4)$$

where “a” stands for activity, and a solution phase activity is distinguished by the use of the subscript “s”. It is evident from equation 3.2 that a mole of either homoionic B- or homoionic A- exchanger is defined as BL_{z_B} and AL_{z_A} respectively, thus equation 3.4 becomes

$$K_a = (a_{B,s}^{z_A} / a_{A,s}^{z_B}) (X_A f_A)^{z_B} (X_B f_B)^{-z_A} = K_v (f_A^{z_B} / f_B^{z_A}) \quad (3.5)$$

where X_i is a cationic mole fraction defined as

$$X_i = n_{iL_{z_i}} / (n_{AL_{z_A}} + n_{BL_{z_B}}) \quad (3.6)$$

f_A , f_B are corresponding rational activity coefficients for the exchange components and the n terms are the number of moles of the appropriate components. K_v is the Vanselow corrected selectivity quotient (i.e. a quotient which contains within itself the correction for solution phase non-ideality Γ (R. M. Barrer et. al (1974)) and which expresses concentrations in the exchanger phase in terms of cationic mole fractions X_i). If the exchanger behaves ideally for all values of X_A , X_B , then it follows that $f_A=f_B=1$ for all X_A , X_B , and (equation 3.5) under such conditions $K_a=K_v$ for all X_A , X_B as expected. However, using equation 3.3 it is equally correct to define K_a as

$$K_a = (a_{B,s}^{z_B} / a_{A,s}^{z_A}) (\alpha_A / \alpha_B)^{z_A z_B} \quad (3.7)$$

where α stands for activity of the appropriate component in the zeolite.

CHAPTER 4

METHODOLOGY AND EXPERIMENTAL STUDIES

4.1 Introduction

In this chapter, the methodology used in the synthesis of the zeolites (LTX, LSX and LTA) is presented. The powder form of each zeolite type after being crushed was packaged and sent to the UK for analysis. Investigations of their efficiency in removing Arsenic and Ammonia from wastewater was tested using ion equilibrium studies. Concentrations of ions before and after treating wastewater with the zeolites were done at the SGS Laboratory Services Ghana Ltd., Tema, Ghana, for Arsenic and the General Chemistry Laboratory of the Faculty of Renewable Natural Resources, KNUST, Kumasi. The synthesis of zeolites, treatment of wastewater, pH and conductivity measurements were done at the Department of Civil Engineering's Water Research laboratory, KNUST, Kumasi.

4.2 Reagents and Apparatus

The following instruments were used during the research. FTIR spectrophotometer (Mattson Instrument, UK), X-ray diffractometer (Philips PW 1710), Thermal analyzer (PerkinElmer), Elemental analyzer (model 1108), SEM (LEO 435 VI), digital pH meter (pH 323), digital electrical conductivity probe, electronic balance, electrical oven, vacuum pump and a rotary shaker (L.E.D Orbit Shaker) . The following reagents were used:

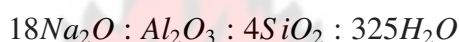
1. Sodium Hydroxide (NaOH) – AnalaR NORMAPUR
2. Sodium Aluminate anhydrous (NaAlO_2) – Sigma-Aldrich
3. Potassium Hydroxide (KOH) – AnalaR NORMAPUR

4. Disodium Metasilicate (Na_2SiO_3) – Aldrich
5. Aluminium Oxide (Al_2O_3) – AnalaR NORMAPUR
6. Distilled Water

4.3 Synthesis of Zeolites

4.3.1 Linde Type X (LTX)

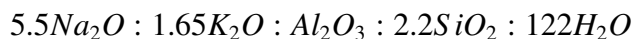
Linde Type X (LTX) of crystal composition: $\text{Na}_{80}[\text{Si}_{112}\text{Al}_{80}\text{O}_{384}]\cdot 260\text{H}_2\text{O}$ was synthesised following the method described by Lechert and Kacirek (1991, 1993) and used by Kwakye-Awuah (2008). The batch composition for the synthesis is given by:



100 g of sodium hydroxide was dissolved in 100 g of distilled water. 97.5 g of alumina powder was added to sodium hydroxide solution while stirring until a homogeneous solution was obtained and allowed to cool. 202.5 g of distilled water was then added to the cooled solution. 219.7 g of sodium silicate was then added to form a gel and stirred for about 30 minutes continuously until a homogeneous gel was obtained. The gel was poured into PTFE-vessels and sealed with aluminium foils, with each vessel containing about 10 g of the gel. The bottles were put into an electric oven at a temperature of 100°C for 8 hours. The reaction in the PTFE bottles was quenched by running cold water on the vessels after they were removed from the oven until they were cooled to room temperature. The synthesized samples were filtered using a vacuum funnel and Whatman No 45 filter paper. The powder samples obtained were washed copiously with distilled water until pH of filtrate was less than 10. Following overnight drying of the powdered zeolite at 100°C in an electrical oven, the zeolite was crushed into uniform powder with pestle and mortar and stored in a plastic bag.

4.3.2 Low Silica Type X (LSX)

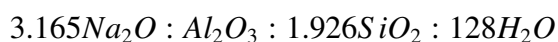
Low-Silica Type X was synthesised following the method described by G. H. Köhl (1987). The batch composition for the synthesis is given by:



22.37 g of sodium aluminate is added to 30 g of distilled water and stirred until all the sodium aluminate was dissolved. In another plastic beaker, 70 g of water was added to 21.53 g of potassium hydroxide and 31.09 g of sodium hydroxide. The mixture was stirred until dissolved. The first solution was then added to the second solution. The solution was then added to 71.8 g of distilled water and 46 g of sodium silicate solution to form a gel. The mixture was stirred until a homogeneous solution was obtained. The gel was poured into PTFE-vessels and sealed with aluminium foils, with each vessel containing about 10 g of the gel. The bottles were put into an electric oven at a temperature of 100 °C for 5 hours. The synthesized samples were diluted with distilled water and filtered using a vacuum funnel and Whatman No. 45 filter paper. The powder samples obtained were washed copiously with 600 ml of 0.01 N NaOH (A.0.1). Following overnight drying of the powdered zeolite at 100 °C in an electrical oven, the zeolite was crushed into uniform powder with pestle and mortar and stored in a plastic bag.

4.3.3 Linde Type A (LTA)

Linde Type A was synthesized following the method described by Thompson and Huber (1982). The batch composition for the synthesis is given by:



0.723 g of sodium hydroxide (Aldrich Chemicals, UK) was dissolved in 80 ml of distilled water. The solution was divided into two equal halves and each transferred into plastic beakers. 8.258 g of sodium aluminate (Sigma-Aldrich, UK) was added to the first halve with continuous stirring until a homogeneous solution was obtained. 15.48 g of disodium metasilicate (Aldrich, UK) was added to other half while mixing until the gel was homogenized. The two samples were mixed quickly and the mixture was again

stirred continuously until a homogeneous solution was obtained. The gel was poured into PTFE-vessels and sealed with aluminium foils, with each vessel containing about 10 g of the gel. The bottles were put into an electric oven at a temperature of 100 °C for 4 hours. The reaction in the PTFE bottles was quenched by running cold water on the vessels after they were removed from the oven until they were cooled to room temperature. The synthesized samples were filtered using a vacuum funnel and Whatman No. 45 filter paper. The powder samples obtained were washed copiously with distilled water until pH of filtrate was less than 9. Following overnight drying of the powdered zeolite at 100 °C in an electrical oven, the zeolite was crushed into uniform powder with pestle and mortar and stored in a plastic bag.

4.4 Characterization of Zeolites

4.4.1 X-ray Diffraction (XRD)

4.4.1.1 Introduction

XRD provides the most comprehensive description of members of zeolite groups. The theory is based on the elastic scattering of X-rays from structures that have long range order. XRD is used to monitor the phase purity and crystallization and the purity of the zeolite particles. XRD also gives information of the particle strain and lattice size

4.4.1.2 Principle of XRD

When a crystal is bombarded with X-rays of a fixed wavelength (similar to spacing of the atomic-scale crystal lattice planes) and at certain incident angles, intense reflected X-rays are produced when the wavelengths of the scattered X-rays interfere constructively (Figure 4.1). In order for the waves to interfere constructively, the differences in the travel path must be equal to integer multiples of the wavelength. When this constructive interference occurs, a diffracted beam of X-rays will leave the crystal at an angle equal to that of the incident beam. The general relationship between the wavelengths of incident X-rays, angle of incidence and spacing between the crystal lattice planes of atoms is known as Bragg's law:

$$n \cdot \lambda = 2d \cdot \sin\theta \quad (4.1)$$

Where: n (an integer) is the “order” of reflection

λ is the wavelength of the incident X-rays

d is the inter-planar spacing of the crystal and

θ is the angle of incidence.

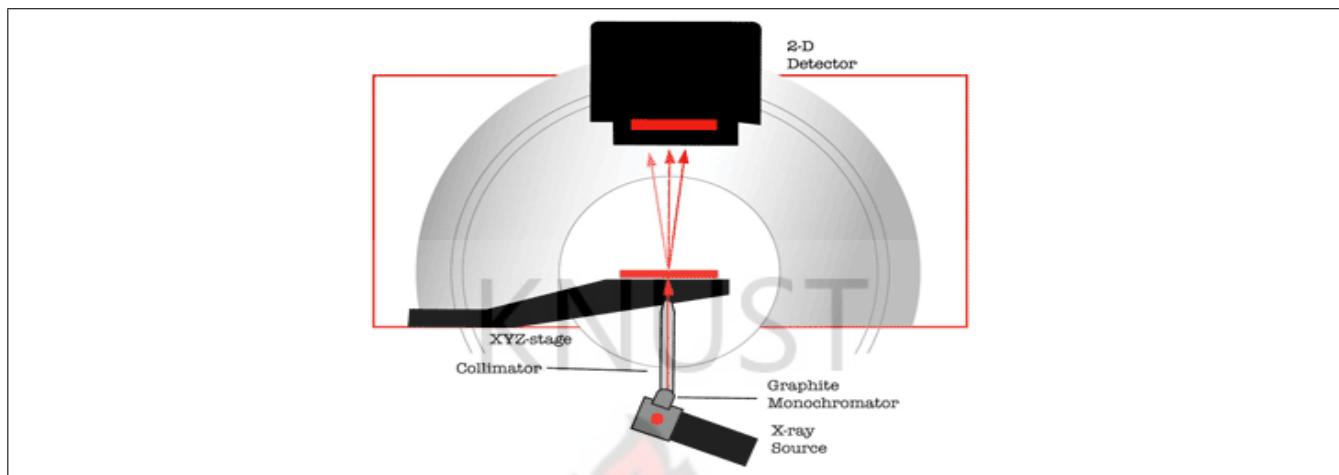


Figure 4.1: Schematic of the X-Ray Diffraction Spectrometer

4.4.1.3 Experimental method

The powder X-ray diffraction patterns of the zeolite samples were recorded on a Philips PW1710 X-ray powder diffractometer over 2θ range of 5° to 55° at a scanning speed of 2° per minute and a step size of 0.05° . The instrument uses sealed Xenon detector. The diffractometer was equipped with graphite monochromated Cu radiation source (8978 eV or $\lambda = 1.5418 \text{ \AA}$). The X-ray source was operated at 40 mA and 40 kV . Data processing was carried out using Philips APD software with a search/match facility and an ICDD database on a DEC Microvax minicomputer interfaced to the diffractometer. The pattern on the computer depends on what is in the sample and by reference to standard data. X-ray powder diffraction patterns of Linde Type X, Linde Type A and Low-Silica Type X were collected on a conventional source using a flat auto plate. Portions of the samples of the three zeolites were placed on the flat auto plate and pressed down to fill the entire perimeter of the plate using a glass plate. After obtaining a smooth and level surface of the powder, the plates were stacked on an automatic sample chamber.

4.4.2 Scanning Electron Microscopy (SEM)

4.4.2.1 Introduction

Scanning Electron Microscopy is a versatile and well-established complementary technique to light optical microscopy. By using a beam of electrons instead of photons, samples can be imaged at far higher magnifications.

4.4.2.2 Principle of SEM

SEM can use different signals to generate contrast mechanisms. The back-scattered electron and secondary electron signals can be used to form images that can give information about the structure, topography and compositional features of a sample.

4.4.2.3 Experimental method

Aluminium stubs were prepared prior to the analysis with an adhesive coating. The samples were sprinkled on the stubs. Where necessary, the samples were gold-coated using an Emscope SC500 Sputter coater to reduce static charging. Electron micrographs were obtained at various magnifications.

4.4.3 Fourier Transformed Infrared Analysis (FTIR)

4.4.3.1 Introduction

FTIR spectroscopy is used to investigate the structural features of samples. Samples of zeolites produced in this study were analyzed with a Mattson FTIR spectrometer (Mattson Instruments, UK) equipped with a ZnSe crystal plate attached to the spectrometer with a mercury cadmium telluride A (MCTA) detector and KBr as beam splitter.

4.4.3.2 Principle of FTIR

The principle of FTIR used in this study is based on the principle of diffuse reflectance. Incident light from a source radiation is scattered in all directions. These spectra can exhibit both absorbance and reflectance features due to contributions from transmission, internal and specular reflectance components, and the scattering phenomena in the collected radiation. A monochromator (usually a salt prism or a grating) separates a source radiation into different wavelengths that are collected by a

slit system. A beam splitter separates the radiation into two: half goes through the sample and half to a reference. A detector collects the radiation that passes through the sample, compares its energy to that going through the reference and sends it to a recorder (computer connected to the instrument). The recorder is calibrated in such a way that it converts the radiation into energy signals which is presented as a function of frequency. Mathematically, the intensity detected of two plane waves, I,

$$I = |\vec{E}|^2 = |E_1|^2 + |E_2|^2 + \vec{E}_1 \cdot 2\vec{E}_2 \cos(\theta) \quad (4.2)$$

Normal incidence, $\theta = kx$ can simplify to

$$I = 2[1 + \cos(kx)] \quad (4.3)$$

For non-monochromatic light;

$$I = \int_0^\infty [1 + \cos(kx)]G(k)dk \quad (4.4)$$

$$= \int_0^\infty G(k)dk + \int_0^\infty G(k) \frac{e^{ikx} + e^{-ikx}}{2} dk \quad (4.5)$$

$$= \frac{1}{2}I(0) + \frac{1}{2} \int_{-\infty}^\infty G(k)e^{ikx} dk \quad (4.6)$$

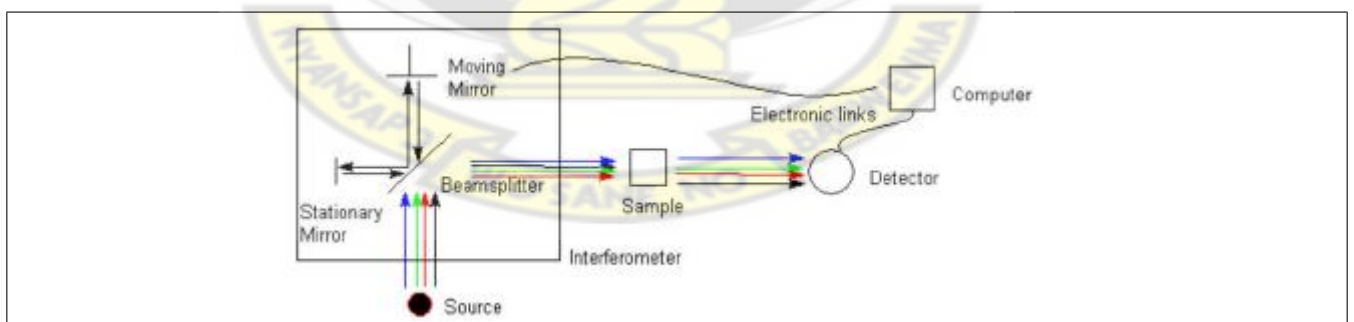


Figure 4.2: Schematic of the FTIR Spectrometer

4.4.3.3 Experimental method

Measurements were done using 100 scans at 4 cm^{-1} resolution, units of $\log(1/R)$ (absorbance), over the mid-IR region of $1200\text{-}400 \text{ cm}^{-1}$. An air background spectrum was collected at the start of the sample collection. A small sample of each zeolite was centered on the ZnSe plate to ensure that it covered the

entire crystal surface, and a pressure clamp was used to apply pressure on the filter. The zeolite samples were analyzed three times for three different samples. A background spectrum was measured before every sample to compensate for atmospheric conditions around the FTIR instrument.

4.5 Analysis of Arsenic in water samples

4.5.1 ICP-OES Analysis

4.5.1.1 Introduction

The concentration of arsenic in water samples from River Nyam was determined by ICP-OES. This analysis was carried out in the laboratory of SGS Laboratory Services Ghana Ltd., Tema, Ghana.

4.5.1.2 Principle of ICP-OES

Figure 4.3 is a schematic presentation of the inductively coupled plasma-optical emission spectrometer. Samples in the form of fluids in argon plasma causing atoms and ions in the plasma vapour are excited into a state of radiated photon emission. The emitted radiation then passes to the spectrometer optic where it is dispersed into its spectral components. The most suitable line of application is measured from the specific wavelength emitted by each atomic element by a charge couple device (CCD). The intensity of radiation is proportional to the concentration of the element within the sample. This is recalculated internally from stored calibration curves and shown directly as a percentage or measured concentration.

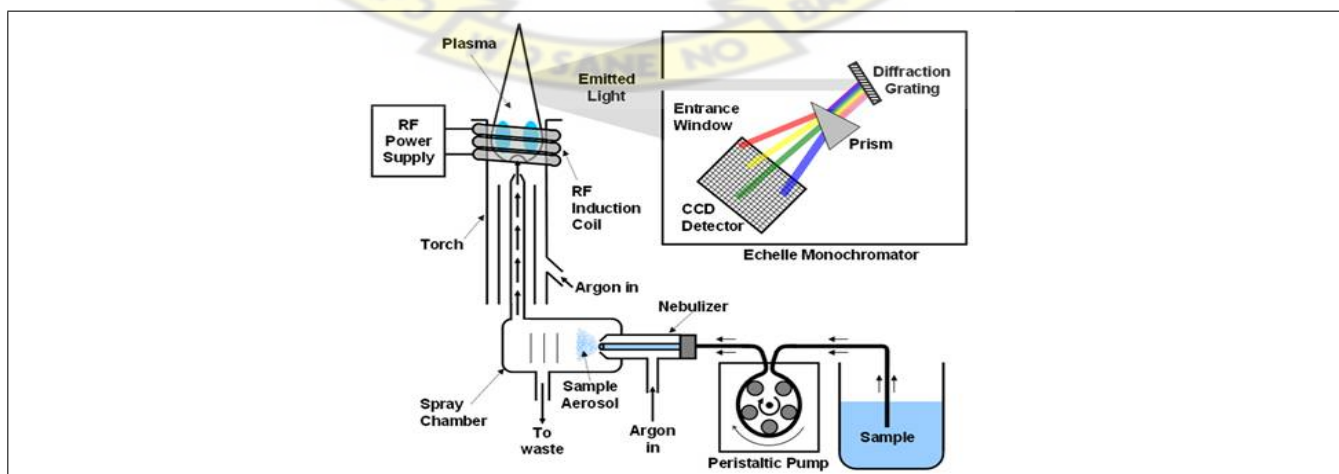


Figure 4.3: Schematic of the ICP-OES

4.5.1.3 Experimental method

200 ml of untreated samples and treated samples preserved with HNO_3 are put into plastic sample bottles and sent to the lab. Samples are then aspirated into an Argon plasma at 8000-10000 K and emit characteristic energy or light as a result of electron transitions through unique energy levels. The emitted light is focused onto a diffraction grating where it is separated into components.

4.6 Analysis of Ammonia in water samples

4.6.1 Photometer

4.6.1.1 Introduction

Ammonia in samples were analysed using the Wagtech Photometer 7100 at the General Chemistry Laboratory of the Institute of Renewable Natural Resources of KNUST, Kumasi, Ghana.

4.6.1.2 Principle of Photometer

A photometer is an instrument for measuring light intensity or optical properties of solutions or surfaces. Most photometers detect the light with photoresistors, photodiodes or photomultipliers. To analyze the light, the photometer may measure the light after it has passed through a filter or through a monochromator for determination at defined wavelengths or for analysis of the spectral distribution of the light. The basic principle of operation of the Wagtech Photometer 7100 is absorption spectroscopy. Absorption spectroscopy is employed as an analytical chemistry tool to determine the presence of a particular substance in a sample and, in many cases, to quantify the amount of the substance present. Absorption lines are typically classified by the nature of the quantum mechanical change induced in the molecule or atom. Rotational lines, for instance, occur when the rotational state of a molecule is changed. Rotational lines are typically found in the microwave spectral region. Vibrational lines correspond to changes in the vibrational state of the molecule and are typically found in the infrared region. Electronic lines correspond to a change in the electronic state of an atom or molecule and are typically found in the visible and ultraviolet region. X-ray absorptions are associated with the excitation of inner shell electrons in atoms. These changes can also be combined (e.g. rotation-vibration transitions), leading

to new absorption lines at the combined energy of the two changes. The energy associated with the quantum mechanical change primarily determines the frequency of the absorption line but the frequency can be shifted by several types of interactions. Electric and magnetic fields can cause a shift. Interactions with neighboring molecules can cause shifts. For instance, absorption lines of the gas phase molecule can shift significantly when that molecule is in a liquid or solid phase and interacting more strongly with neighboring molecules. Absorption lines are often depicted as infinitesimally thin lines, i.e., delta functions, but observed lines always have a shape that is determined by the instrument used for the observation, the material absorbing the radiation and the physical environment of that material. It is common for lines to have the shape of a Gaussian or Lorentzian distribution. It is also common for a line to be characterized solely by its intensity and width instead of the entire shape being characterized. The integrated intensity—obtained by integrating the area under the absorption line—is proportional to the amount of the absorbing substance present. The intensity is also related to the temperature of the substance and the quantum mechanical interaction between the radiation and the absorber. This interaction is quantified by the transition moment and depends on the particular lower state the transition starts from and the upper state it is connected to. The width of absorption lines may be determined by the spectrometer used to record it. A spectrometer has an inherent limit on how narrow a line it can resolve and so the observed width may be at this limit. If the width is larger than the resolution limit, then it is primarily determined by the environment of the absorber. A liquid or solid absorber, in which neighboring molecules strongly interact with one another, tends to have broader absorption lines than a gas. Increasing the temperature or pressure of the absorbing material will also tend to increase the line width. It is also common for several neighboring transitions to be close enough to one another that their lines overlap and the resulting overall line is therefore broader yet.

4.6.1.3 Experimental method

The Photometer measures the amount of ammoniacal nitrogen present in the sample and the result is multiplied by a factor of 1.2 to obtain the amount of ammonia present in the sample.

10 ml of the sample was put into a glass crucet and the Palintest Ammonia Tablet No.1 and Palintest Ammonia Tablet No.2 were added, crushed and stirred till all was dissolved. The solution was allowed

to stand for 10 minutes and then placed into photometer.

The result on the LCD of the photometer was recorded and this was repeated for all samples both treated and untreated.

4.7 Kinetic Studies

4.7.1 Wastewater Sampling

Water samples were initially collected from four sources: Rivers Birim (Kyebi), Jimi (Obuasi), Nyam (Obuasi) and Wewe (Kumasi - KNUST). These samples were then analysed for their arsenic concentrations. The river with the highest arsenic concentration, that is, Nyam was chosen to be used as wastewater to be treated for Arsenic contamination. For Ammonia removal, the water samples from Nyam contained negligible amounts of ammonia thus two new samples were collected from the KNUST Waste Treatment Center. These samples contained significantly high concentrations of ammonia and thus were used for ammonia removal.

4.7.2 Batch Technique

The batch technique was utilised to monitor the effect of contact time on ion exchange. An equal volume of 100 ml of water samples was measured into conical flasks. The ratio of zeolite to water sample was 1.5 g of Zeolite : 100 ml of water sample for arsenic removal and 0.8 g of zeolite : 50 ml of water sample for ammonia removal. The mass of zeolite to volume of sample ratio is very important since pH affects the efficiency of the adsorbent. Therefore with the reduction in sample volume it is imperative to reduce the mass of zeolite adsorbent equally. With varying time labels, the flasks were placed on a rotary shaker at an average speed of 200 rpm at room temperature. Time intervals were 30, 60 and 90 minutes. The zeolite was then separated from the supernatant at the required time. Each sample was filtered using Whatman Filter No. 45 paper. The pH and conductivity of each water sample was recorded before and after treatment. The concentrations of arsenic and ammonia in the water samples were determined using an ICP-OES and a Wagtech Photometer. This was to determine the optimum time for treatment. All tests were repeated using the optimum time of 30 minutes for arsenic removal. The percentage removal

efficiency of each zeolite was determined using sorption isotherms.

4.8 Sorption Isotherms

The analysis of the isotherm data is important to develop an equation which accurately represents the results and which could be used for design purposes. In order to investigate the sorption isotherm, two equilibrium models were analysed: Langmuir and Freundlich isotherm equations. The Langmuir model is obtained under the ideal assumption of a totally homogeneous adsorption surface, whereas the Freundlich isotherm is suitable for a highly heterogeneous surface (Hui et al., 2005).

4.8.1 Langmuir Isotherm

The Langmuir sorption isotherm is the best known of all isotherms describing sorption and it has been successfully applied to many sorption processes (Hui et al., 2005). It is represented as:

$$q_e = q_m \frac{bC_e}{1 + bC_e} \quad (4.7)$$

Alternatively, the equation can be manipulated to linear form as:

$$\frac{1}{q_e} = \frac{1}{q_m b} \times \frac{1}{C_e} + \frac{1}{q_m} \quad (4.8)$$

which gives

$$\frac{C_e}{q_e} = \frac{1}{q_m} C_e + \frac{1}{q_m b} \quad (4.9)$$

Where C_e is the equilibrium aqueous metal ions concentration (mg l^{-1}), q_e is the amount of metal ions adsorbed per gram of adsorbent at equilibrium (mg g^{-1}), q_m and b are the Langmuir constants related to the maximum adsorption capacity and energy of adsorption, respectively. The values of q_m (mg g^{-1}) and b (mg^{-1}) can be determined from the linear plot of C_e/q_e versus C_e . Thus,

$$q_m = \frac{1}{\text{slope}} \quad (4.10)$$

and

$$b = \frac{\text{slope}}{y - \text{intercept}} \quad (4.11)$$

4.8.2 Freundlich Isotherm

The Freundlich isotherm is most frequently used to describe the adsorption of inorganic and organic components in solution (Hui et al., 2005). This fairly satisfactory empirical isotherm can be used for a non-ideal sorption that involves heterogeneous sorption and is expressed as:

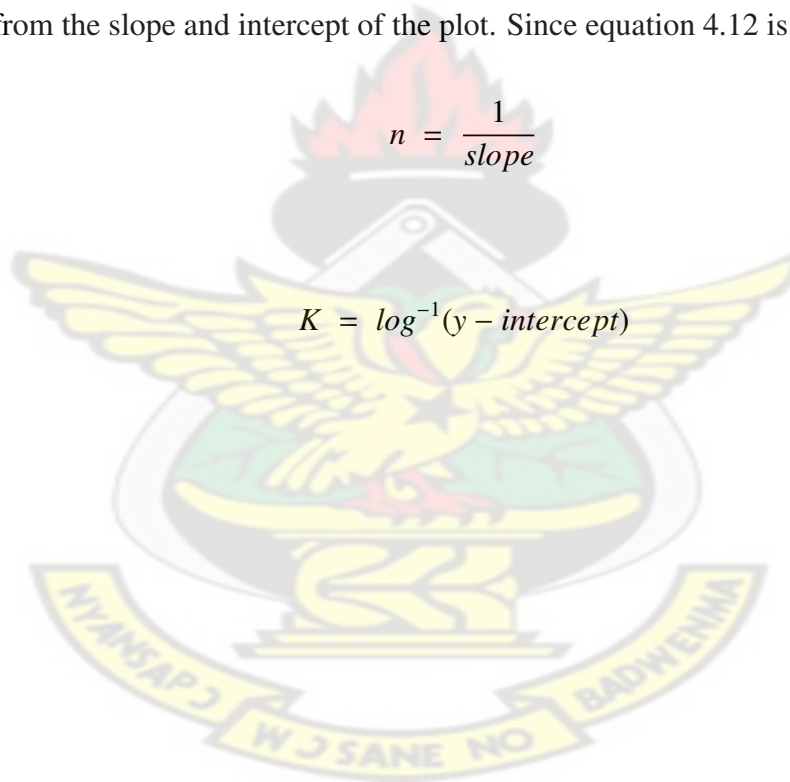
$$\log q_e = \log K + \frac{1}{n} \log C_e \quad (4.12)$$

where K is roughly an indicator of the adsorption capacity and $1/n$ the adsorption intensity. The magnitude of the exponent $1/n$ gives an indication of the favourability of adsorption. Values of n , where $n > 1$ represent favourable adsorption condition. By plotting $\log q_e$ versus $\log C_e$, values of K and n can be determined from the slope and intercept of the plot. Since equation 4.12 is a linear then

$$n = \frac{1}{\text{slope}} \quad (4.13)$$

and

$$K = \log^{-1}(y - \text{intercept}) \quad (4.14)$$



CHAPTER 5

RESULTS AND DISCUSSIONS

In this chapter the results based on the synthesis and the characterization of zeolites and treatment of water samples for the removal of Arsenic and Ammonia are presented.

Synthesis and characterisation of Zeolites

5.1 Synthesis and characterisation of Linde Type X

5.1.1 Synthesis

As discussed in 4.3.1, the batch composition for the synthesis is given by:



Two unsuccessful attempts were initially made in synthesising LTX, the third attempt, however, was successful.

5.1.2 Characterisation

The SEM micrographs in Figure 5.1 confirmed the phase purity of the crystal morphology and similar to those of known literature. Crystals varied between 2–10 μm .

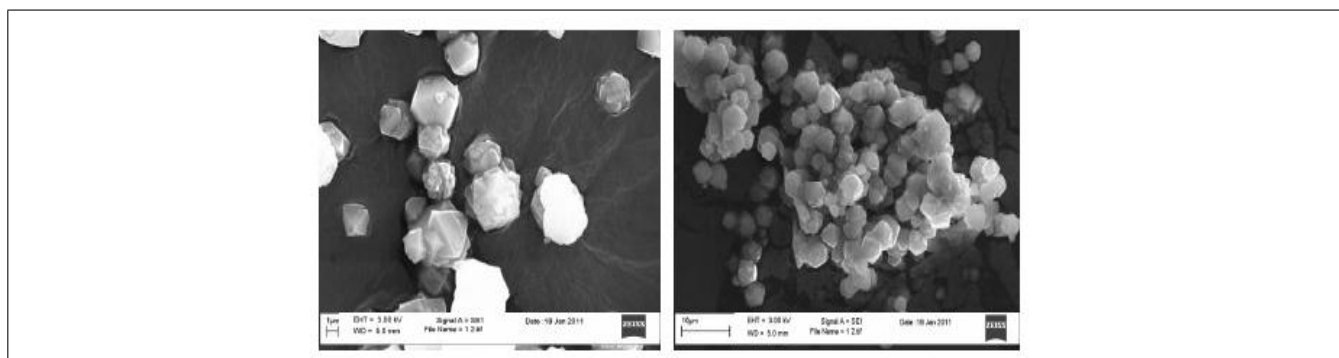


Figure 5.1: SEM Micrographs of LTX

XRD analysis was carried on LTX to monitor the phase purity and crystallization and the purity of the final product. As cited in Kwakye-Awuah (2008), the XRD pattern of LTX samples must accord with the ICDD standard reference pattern in order to be validated as an as-synthesized LTX. Highly crystalline crystals were obtained as shown by the reflection peaks (Figure 5.2). The presence of amorphous material is characterized by small zig-zag peaks. Strong peaks confirm full crystallization.

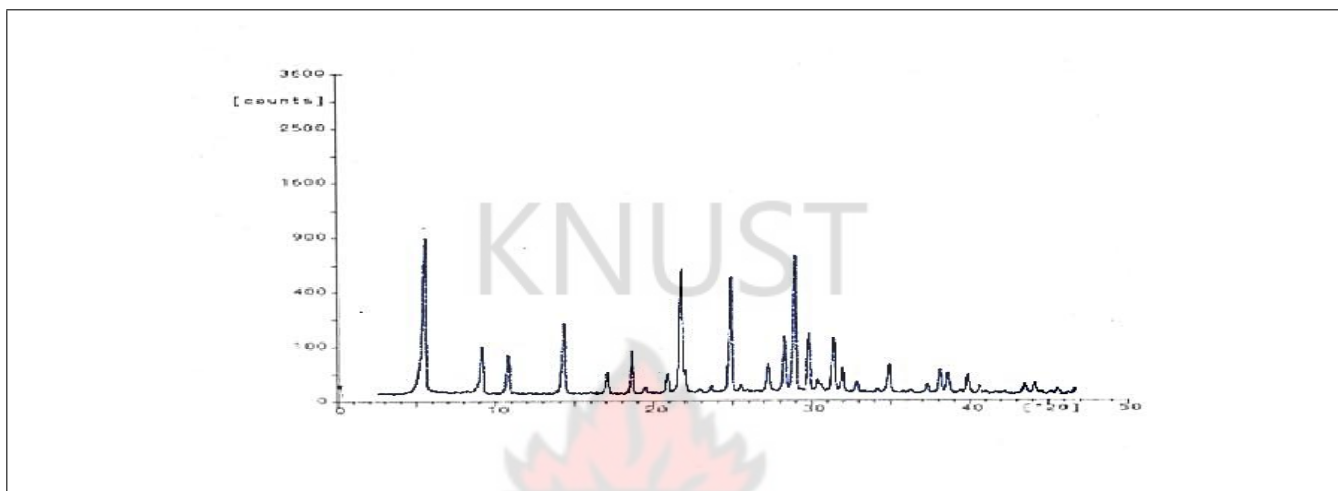


Figure 5.2: XRD of Linde Type X

Structural characterisation of the zeolite was done by FTIR to confirm the formation of the zeolite. Although every zeolite has its characteristic FTIR pattern some common features are observed for all zeolites.

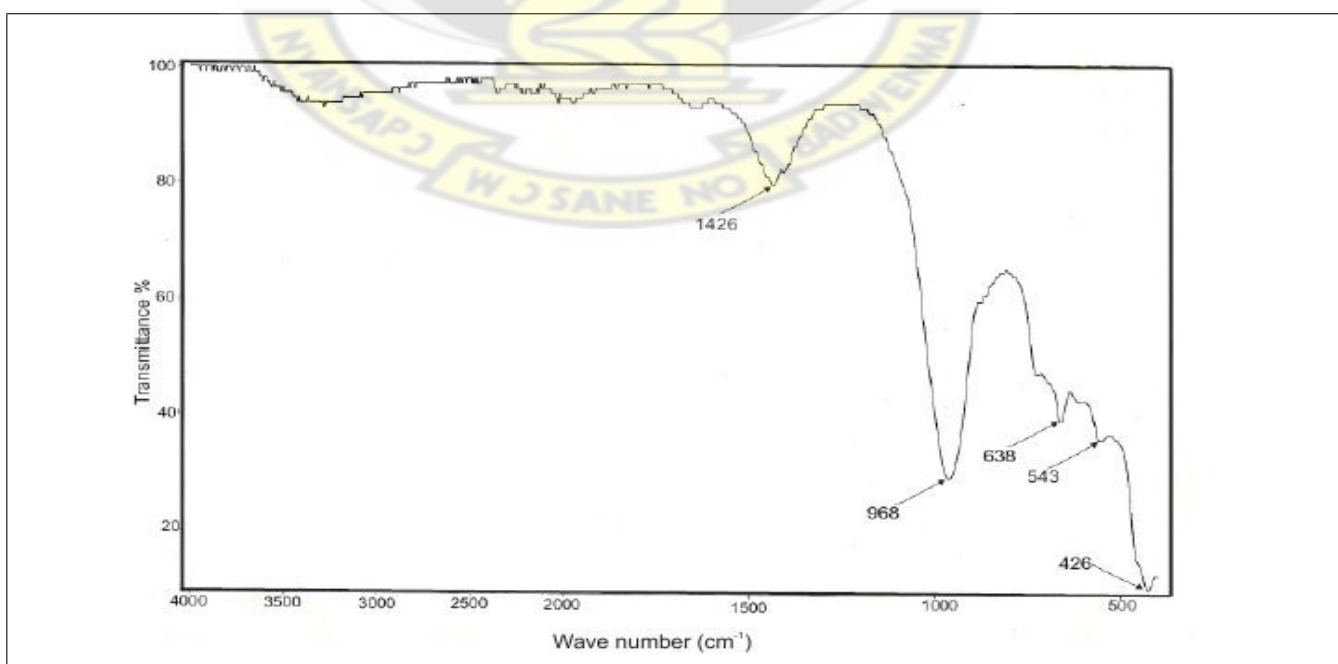


Figure 5.3: FTIR Spectra of LTX

The characteristic peaks of the FTIR spectrum were exhibited at 1426 cm^{-1} and 968 cm^{-1} . Vibrations associated with double rings of the external T–O linkages occurred at 638 cm^{-1} . Asymmetric stretching due to the internal vibrations of the framework tetrahedra occurred at 968 cm^{-1} and the band at 426 cm^{-1} . The general infrared assignments in zeolites as proposed by Flanigen et al., (1978) and Mozgawa, (2000) and cited by Kwakye-Awuah (2008) are presented in Table 5.1.

Table 5.1 General Infrared Assignments

Internal Vibrations	
Asymmetric Stretch	1250 – 950
Symmetric stretch	720 – 650
T– O Bend	500 – 420
External T–O Linkages	
Double ring	650 – 500
Pore opening	420 – 300
Symmetric stretch	750 – 820
Asymmetric stretch	1150 – 1050

5.2 Synthesis and characterisation of Low Silica Type X

5.2.1 Synthesis

As discussed in 4.3.2, the batch composition for the synthesis is given by:



Synthesis of Low-Silica Type X was successful in the first attempt.

5.2.2 Characterisation

SEM micrographs of LSX showed an intergrowth of fine octahedral crystallites of submicron size and were closely similar in size and appearance with fairly uniform morphology.

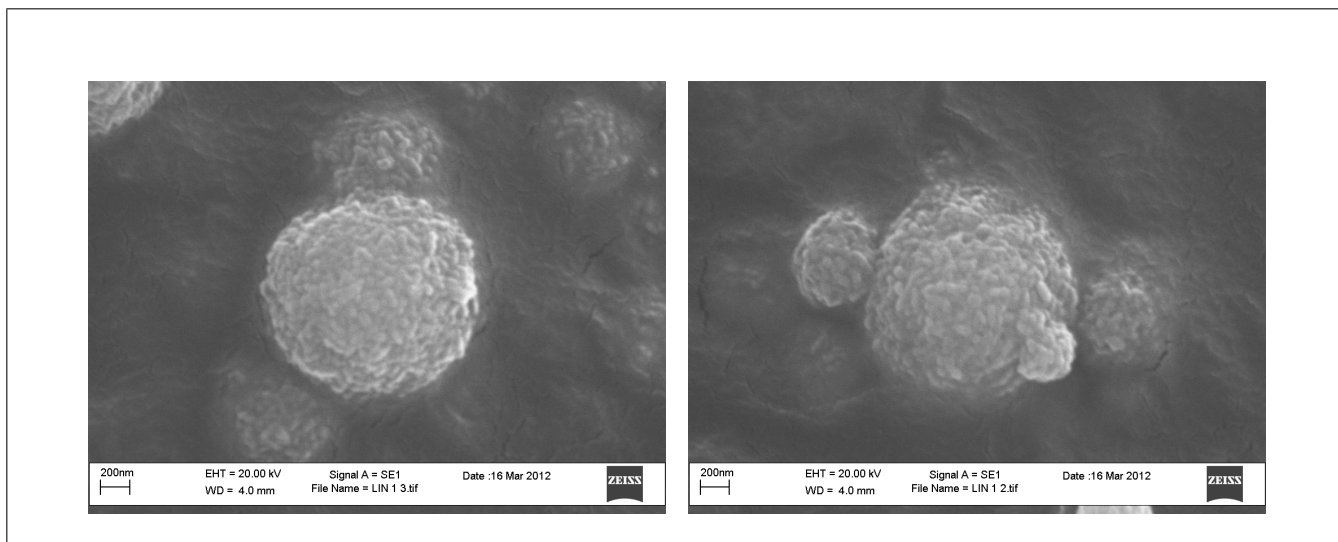


Figure 5.4: SEM Micrographs of Low-Silica Type X.

Highly crystalline crystals were obtained as shown by the XRD reflection peaks (Figure 5.5) with the first peak appearing between 6 - 10 °. There were also no other phases of impurities present in the crystals. Hence the purity of the zeolite was validated.

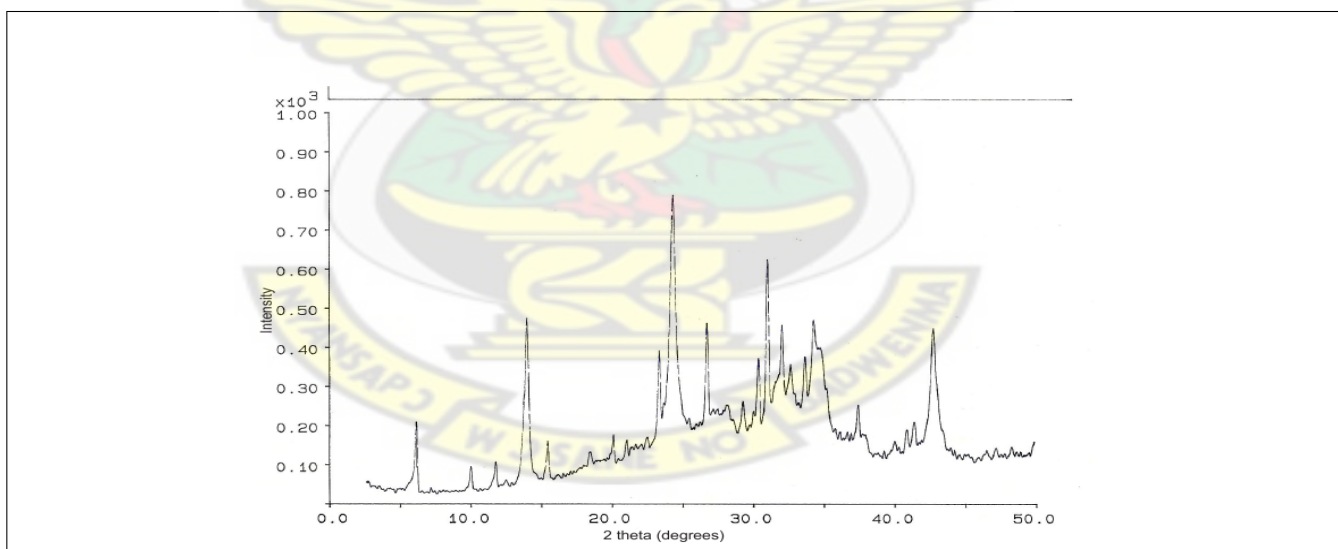


Figure 5.5: XRD Diffraction Patterns of LSX

Figure 5.6 is the FTIR spectra of LSX. A large band was observed at 962 cm^{-1} which can be attributed to the overlapping of the asymmetric vibrations of Si-O (bridging) and Si-O⁻ (non-bridging) bonds. Vibrations associated with double rings occurred at 615 cm^{-1} and 548 cm^{-1} . Symmetric stretching associated with internal vibrations occurred at 664 cm^{-1} and the band at 423 cm^{-1} is assigned to the

vibrations due to the bending of the T–O tetrahedra.

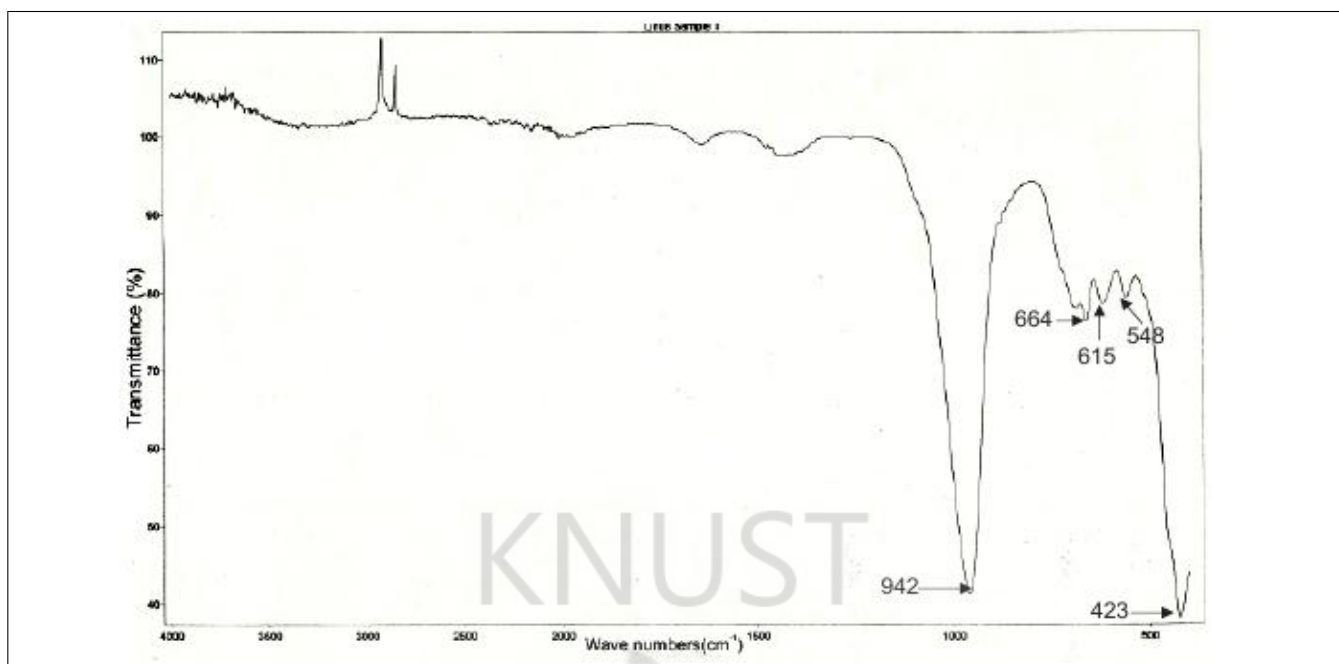


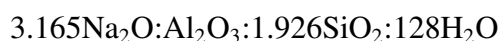
Figure 5.6: FTIR Spectra of LSX

Thermogravimetric measurements were conducted heating from 50.00 °C to 960.00 °C at 20.00 °C/minute. Results show that there was a rapid decrease in weight percentage between 50.00 °C and 300.00 °C (Figure A.2).

5.3 Synthesis and characterisation of Linde Type A

5.3.1 Synthesis

As discussed in 4.3.3, the batch composition for the synthesis is given by:



Linde Type A was obtained in the first attempt of synthesis.

5.3.2 Characterisation

SEM micrographs showed that LTA an intergrowth of typical cubic crystallites of and confirmed crystal morphology (Figure 5.7). This can be seen in the similar particle size and appearance.

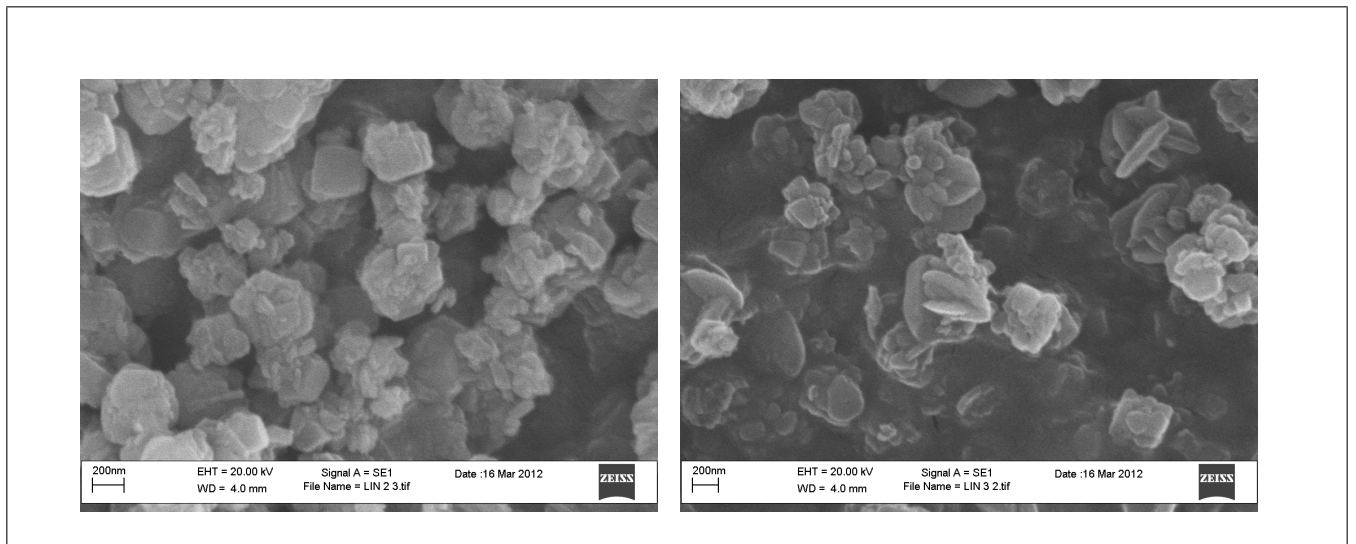


Figure 5.7: SEM micrographs of Linde Type A.

XRD analysis of the zeolite, Figure 5.8 was validated by known literature. The first peak appears between $6 - 10^\circ$ and shows no impurity phases.

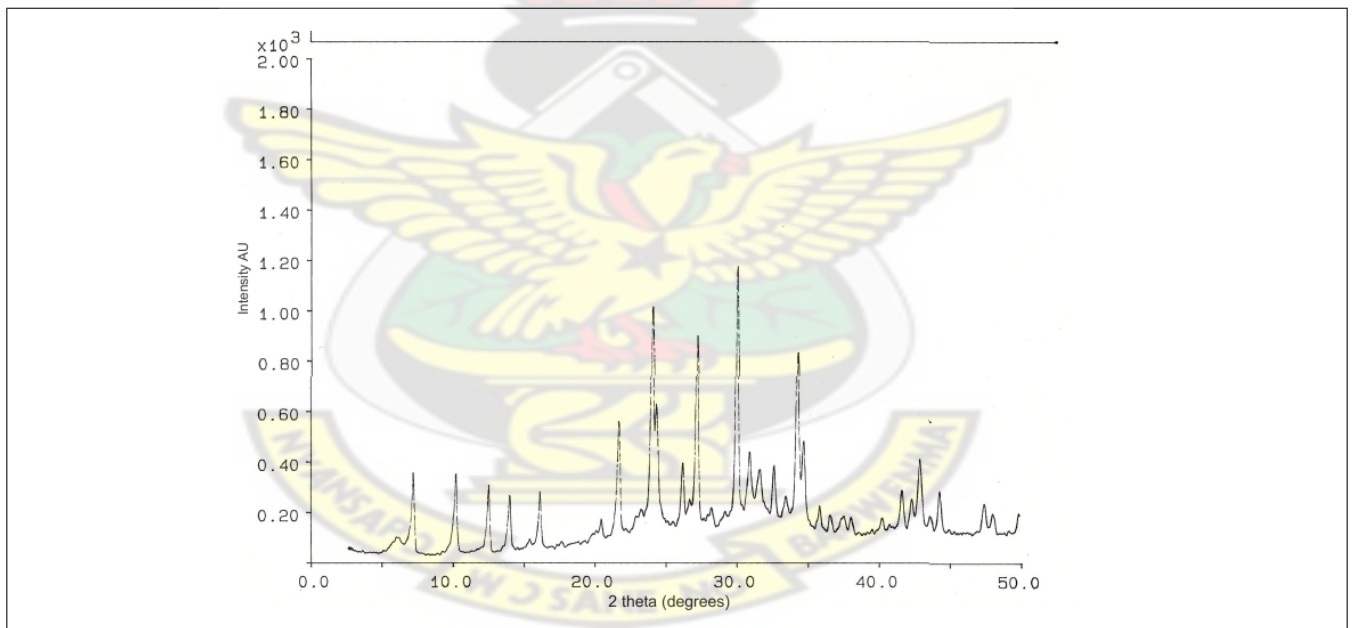


Figure 5.8: Diffraction Pattern of LTA

The FTIR spectra of LTA is given in Figure 5.9. The band attributed to the overlapping of the asymmetric vibrations of Si–O (bridging) and Si–O (non-bridging) bonds occurred at 971 cm^{-1} . Vibrations associated with double rings occurred at 558 cm^{-1} and 519 cm^{-1} whilst the band at 442 cm^{-1} is the vibrations due to the bending of the T–O tetrahedra.

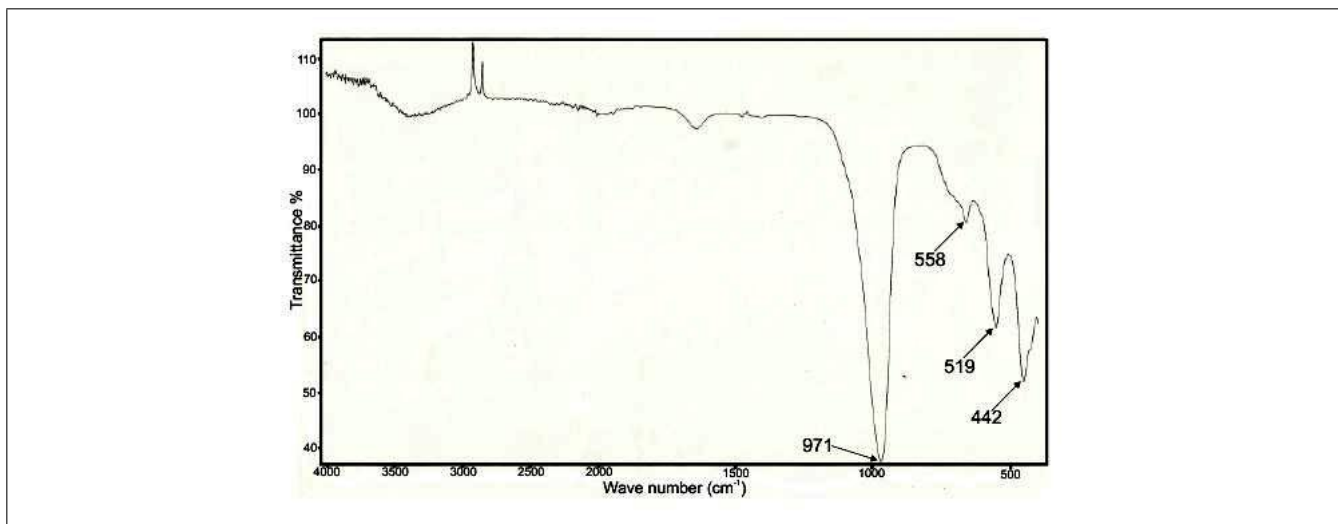


Figure 5.9: FTIR Spectra of LTA

Thermogravimetric measurements were conducted heating from 50.00 °C to 960.00 °C at 20.00 °C/minute. Results also show that there was a rapid decrease in weight percentage between 50.00 °C and 300.00 °C (Figure A.3).

Analysis of Arsenic and Ammonia removal from samples by Zeolites

5.4 Analysis of Arsenic removal from samples by Zeolites

5.4.1 Kinetics

River Nyam was selected based on the measured amounts of Arsenic found in its samples. Samples from Rivers Birim (Kyebi), Jimi (Obuasi) and Wewe (KNUST Campus, Kumasi) were also collected to determine their Arsenic concentrations. Results are in the appendix .

From kinetics studies, the optimum time of 30 minutes was chosen for treatment. Table 5.2 gives the measured concentrations and removal capacities of the zeolites with respect to time intervals of 30 minutes, 60 minutes and 90 minutes using zeolite Linde Type X (LTX) only for two water samples (Appendix A.4).

Table 5.2 Kinetics of Optimum Treatment Time

Time	Equilibrium Concentration of Arsenic (mg/l)	Removal Efficiency (%)	Sorption Capacity
Sample 1			
0 mins	0.15	0	0
30 mins	0.028	81.35	8.133
60 mins	0.044	70.67	7.067
90 mins	0.014	90.67	9.667
Sample 2			
0 mins	0.19	0	0
30 mins	0.042	77.89	9.867
60 mins	0.076	60.00	7.6
90 mins	0.060	68.42	8.67

5.4.2 Sample 1 - NYAM 1

Sample 1 was collected from River Nyam on 23rd August, 2011, and subsequently treated in the lab.

Untreated and treated samples were analysed using ICP–OES.

Table 5.3 Results of Treatment of Sample 1 for Arsenic Removal

	Equilibrium Concentration of Arsenic (mg/l)	Removal Efficiency (%)	Sorption Capacity
Initial Concentration	0.15	0	0
Treatment with LTX	0.028	81.35	8.133
Treatment with LSX	0.022	85.33	8.533
Treatment with LTA	0.006	96.00	9.6

5.4.3 Sample 2 - NYAM 2

Sample 2 was collected from River Nyam on 21st September, 2011, and subsequently treated in the lab.

Untreated and treated samples were analysed using ICP–OES.

Table 5.4 Results of Treatment of Sample 2 for Arsenic Removal

	Equilibrium Concentration of Arsenic (mg/l)	Removal Efficiency (%)	Sorption Capacity
Initial Concentration	0.19	0	0
Treatment with LTX	0.042	77.89	9.867
Treatment with LSX	0.026	86.31	10.933
Treatment with LTA	0.032	83.16	10.533

5.4.4 Sample 3 - NYAM 3

Sample 3 was collected from River Nyam on 22nd October, 2011, and subsequently treated in the lab.

Untreated and treated samples were analysed using ICP–OES.

Table 5.5 Results of Treatment of Sample 3 for Arsenic Removal

	Equilibrium Concentration of Arsenic (mg/l)	Removal Efficiency (%)	Sorption Capacity
Initial Concentration	0.28	0	0
Treatment with LTX	0.09	67.86	12.667
Treatment with LSX	0.09	67.86	12.667
Treatment with LTA	0.050	82.14	15.333

5.4.5 Sample 4 - NYAM 4

Sample 4 was collected from River Nyam on 15th November, 2011, and subsequently treated in the lab.

Untreated and treated samples were analysed using ICP–OES.

Table 5.6 Results of Treatment of Sample 4 for Arsenic Removal

	Equilibrium Concentration of Arsenic (mg/l)	Removal Efficiency (%)	Sorption Capacity
Initial Concentration	0.32	0	0
Treatment with LTX	0.072	77.50	16.533
Treatment with LSX	0.09	71.87	15.333
Treatment with LTA	0.09	71.87	15.333

5.4.6 Sample 5 - NYAM 5

Sample 5 was collected from River Nyam on 7th December, 2011, and subsequently treated in the lab. Untreated and treated samples were analysed using ICP–OES.

Table 5.7 Results of Treatment of Sample 5 for Arsenic Removal

	Equilibrium Concentration of Arsenic (mg/l)	Removal Efficiency (%)	Sorption Capacity
Initial Concentration	0.20	0	0
Treatment with LTX	0.062	69.00	9.2
Treatment with LSX	0.032	84.00	11.2
Treatment with LTA	0.032	84.00	11.2

It was also noted that the amount of arsenic in the raw water samples for the period generally increased. The River Nyam being near a tailings disposal site of AngloGold Ashanti Company in Obuasi, it is possible that some amount of arsenic leached into it. It is suggested that since the period of collection of sample was from the end of the raining season into the dry season, the initial samples were as a result of dilution of the river and as the rains stopped the apparent increase in arsenic content in the river. Samples were however taken at the same point along the river.

5.5 Analysis of Ammonia removal from samples using LTA

For Ammonia removal, samples collected from the River Nyam when tested for ammonia had negligible amounts of Ammonia so samples for Ammonia removal were collected from the KNUST Wastewater Treatment Centre. LTA only was used for the removal of Ammonia due to time and financial constraints. LTA was chosen due to its better removal efficiencies exhibited when used in arsenic removal. The use of one zeolite adsorbent was due to time and financial constraints.

5.5.1 Sample 1

Sample 1 was influent collected from the Treatment centre.

Table 5.8 Results of Treatment 1 of Sample 1 for Ammonia Removal

	Equilibrium Concentration of Ammonia (mg/l)	Removal Efficiency (%)	Sorption Capacity
Initial Concentration	0.72	0	0
Treatment for 30 minutes	0.168	76.67	34.50
Treatment for 60 minutes	0.336	53.33	24.00
Treatment for 90 minutes	0.504	30.00	13.50

Table 5.9 Results of Treatment 2 of Sample 1 for Ammonia Removal

	Equilibrium Concentration of Ammonia (mg/l)	Removal Efficiency (%)	Sorption Capacity
Initial Concentration	0.72	0	0
Treatment for 30 minutes	0.06	91.67	41.25
Treatment for 60 minutes	0.384	41.67	21.00
Treatment for 90 minutes	0.36	50.00	22.50

Table 5.10 Results of Treatment 3 of Sample 1 for Ammonia Removal

	Equilibrium Concentration of Ammonia (mg/l)	Removal Efficiency (%)	Sorption Capacity
Initial Concentration	0.72	0	0
Treatment for 30 minutes	0.06	91.67	41.25
Treatment for 60 minutes	0.36	50.00	22.50
Treatment for 90 minutes	0.336	53.33	24.00

Table 5.11 Results of Treatment 4 of Sample 1 for Ammonia Removal

	Equilibrium Concentration of Ammonia (mg/l)	Removal Efficiency (%)	Sorption Capacity
Initial Concentration	0.72	0	0
Treatment for 30 minutes	0.048	93.33	42.00
Treatment for 60 minutes	0.528	26.67	12.00
Treatment for 90 minutes	0.336	53.33	24.00

For Sample 1, the results show that the best time for ammonia removal was within 30 minutes, after which, leaching of ammonia from the zeolite back into the solution. Thus, the gradual increase in

ammonia as time increased.

5.5.2 Sample 2

Sample 2 was sludge collected from the treatment centre.

Table 5.12 Results of 1st sample of Sample 2 for Ammonia Removal

	Equilibrium Concentration of Ammonia (mg/l)	Removal Efficiency (%)	Sorption Capacity
Initial Concentration	0.52	0	0
Treatment for 30 minutes	0.108	79.23	25.75
Treatment for 60 minutes	0.048	90.77	29.50
Treatment for 90 minutes	0.492	5.38	1.75

Table 5.13 Results of 2nd sample of Sample 2 for Ammonia Removal

	Equilibrium Concentration of Ammonia (mg/l)	Removal Efficiency (%)	Sorption Capacity
Initial Concentration	0.52	0	0
Treatment for 30 minutes	0.096	81.54	26.50
Treatment for 60 minutes	0.048	90.77	29.50
Treatment for 90 minutes	0.48	7.69	2.50

Table 5.14 Results of 3rd sample of Sample 2 for Ammonia Removal

	Equilibrium Concentration of Ammonia (mg/l)	Removal Efficiency (%)	Sorption Capacity
Initial Concentration	0.52	0	0
Treatment for 30 minutes	0.096	81.54	26.50
Treatment for 60 minutes	0.06	88.46	28.75
Treatment for 90 minutes	0.432	16.92	5.5

Table 5.15 Results of 4th sample of Sample 2 for Ammonia Removal

	Equilibrium Concentration of Ammonia (mg/l)	Removal Efficiency (%)	Sorption Capacity
Initial Concentration	0.52	0	0
Treatment for 30 minutes	0.084	83.85	27.25
Treatment for 60 minutes	0.072	86.15	28.00
Treatment for 90 minutes	0.492	5.38	1.75

5.6 Sorption Isotherms

The analysis of the isotherm data is important to develop an equation which accurately represents the results and which could be used for design purposes. The Langmuir sorption isotherm has been successfully applied to many sorption processes (Hui et al., 2005). The Freundlich sorption isotherm is also used in this work. This will give us the opportunity to compare which of the models this data fits well.

5.6.1 Linde Type X (LTX)

This zeolite was used only for the removal of the arsenic and not applied for ammonia removal. For Ammonia removal, due to time and financial constraints LTX and LSX could not be synthesised. However, since LTA performed better than the other zeolites, LTA was used. The graph plotted from the equilibrium concentration/sorption capacity versus equilibrium concentration was used to find the Langmuir constants; the maximum adsorption capacity (q_m) and energy of adsorption (b); and $\log C_e$ versus $\log q_e$ were plotted to obtain the Freundlich constants adsorption capacity, K and adsorption intensity, $1/n$. The slope of both models showed similar behaviours, increasing proportionally. R^2 values obtained decreased from 0.594 for the Langmuir model to 0.508 for the Freundlich model.

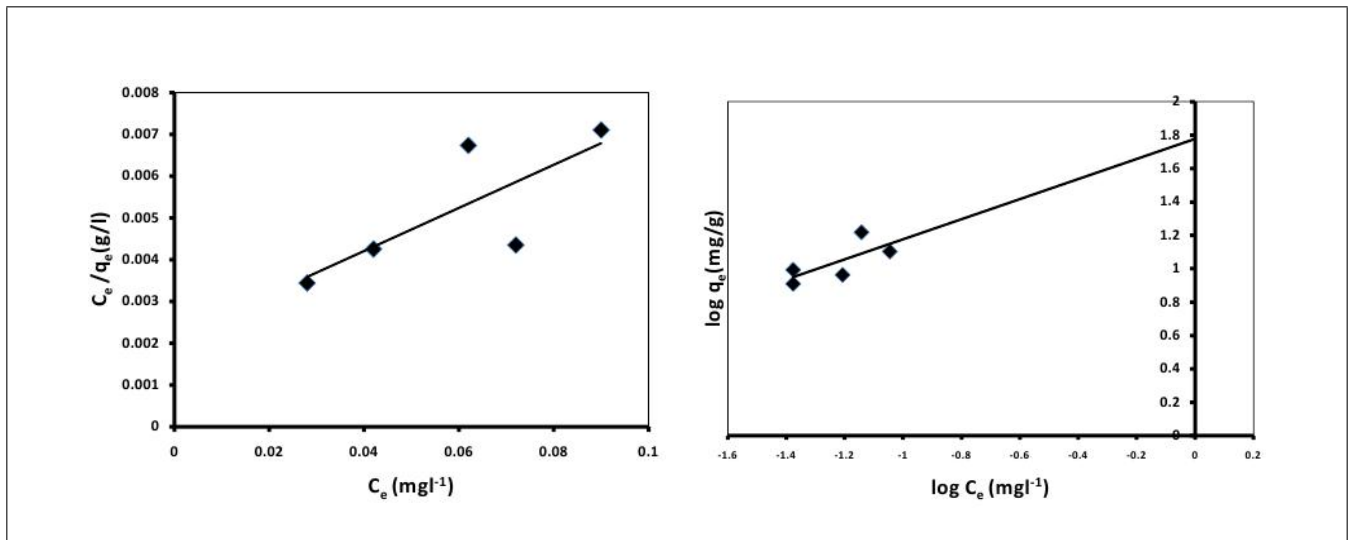


Figure 5.10: (a) Langmuir isotherm model and (b) Freundlich isotherm model of LTX.

5.6.2 Low Silica Type X

LSX was also only used for the removal of arsenic. The slopes also showed similar behaviours for both models - proportional increases as for LTX. The Langmuir constants q_m and b as well as the Freundlich constants K and $1/n$. R^2 values of the Freundlich model also decreased as compared to that of the Langmuir model.

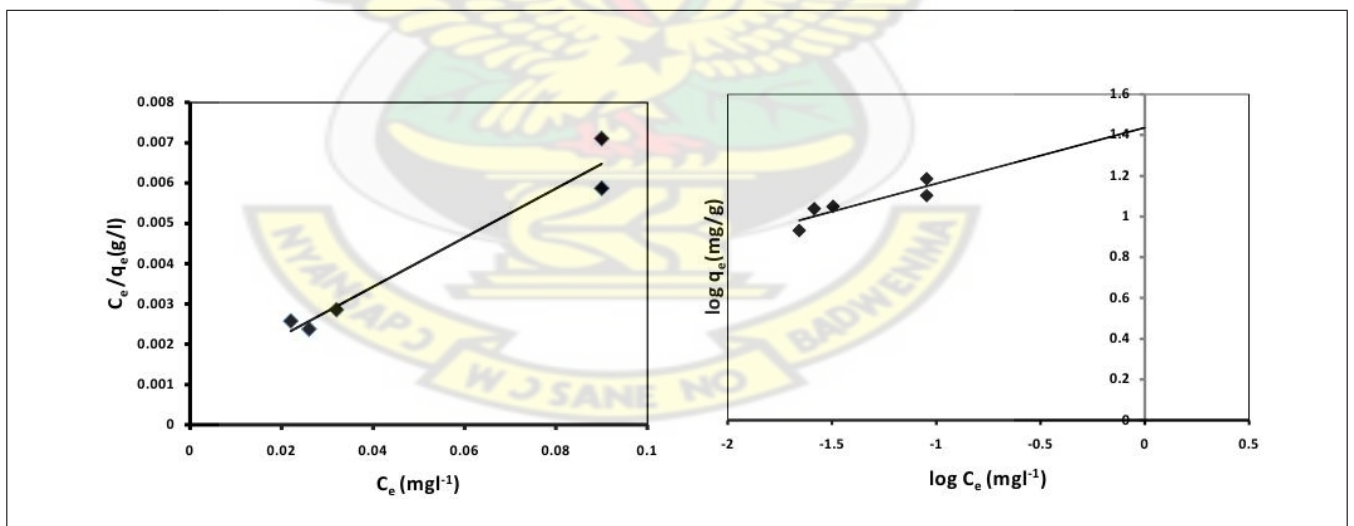


Figure 5.11: (a) Langmuir isotherm model and (b) Freundlich isotherm model of LSX.

5.6.3 Linde Type A

Arsenic removal

The models also showed similar characteristics as LTX and LSX. The Langmuir constants q_m and b as well as the Freundlich constants K and $1/n$. R^2 values of the Freundlich model also decreased as

compared to that of the Langmuir model.

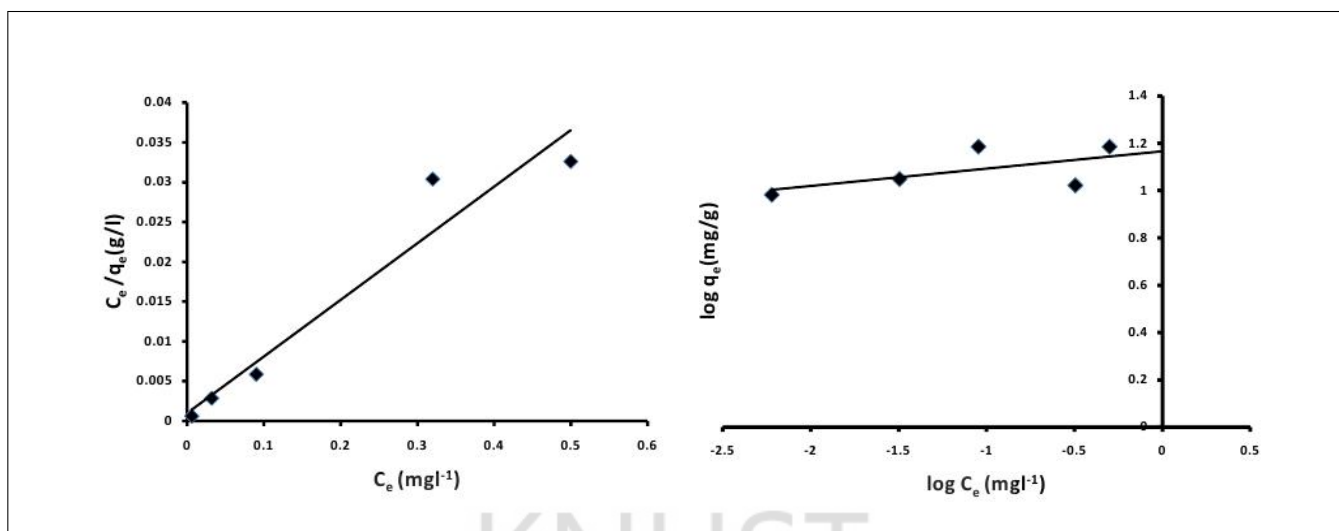


Figure 5.12: (a) Langmuir isotherm model and (b) Freundlich isotherm model of LTA.

Ammonia removal

For ammonia removal, a negative slope was obtained though it was also proportional. However, R^2 values of the Freundlich model this time increased as compared to that of the Langmuir model

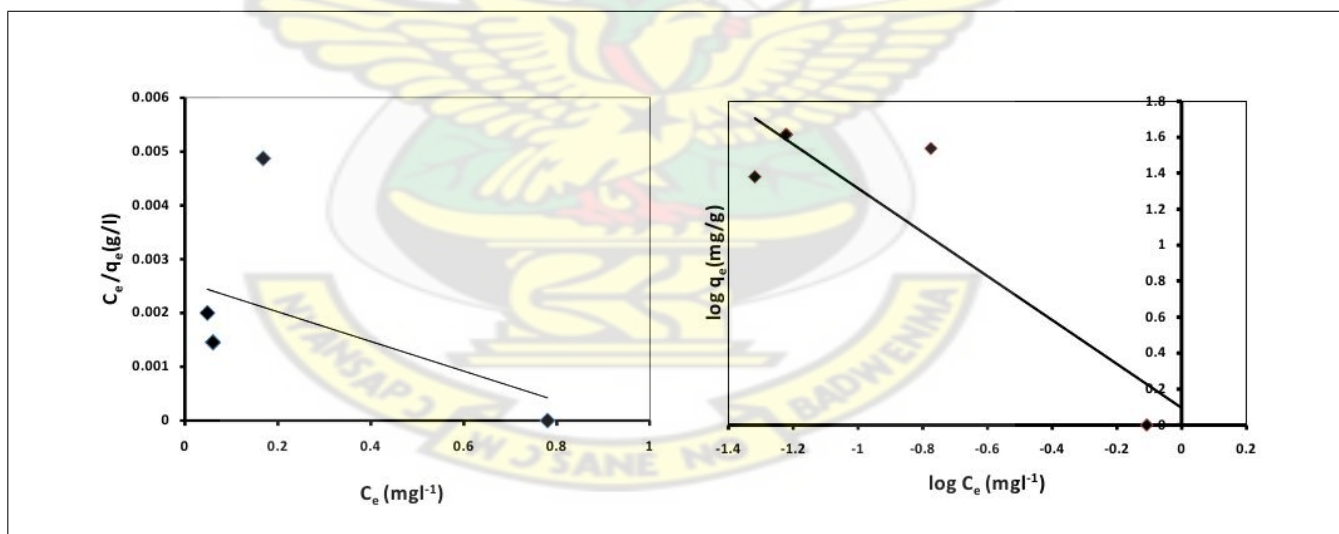


Figure 5.13: (a) Langmuir isotherm model and (b) Freundlich isotherm model of LTA for Ammonia treatment for 30 minutes.

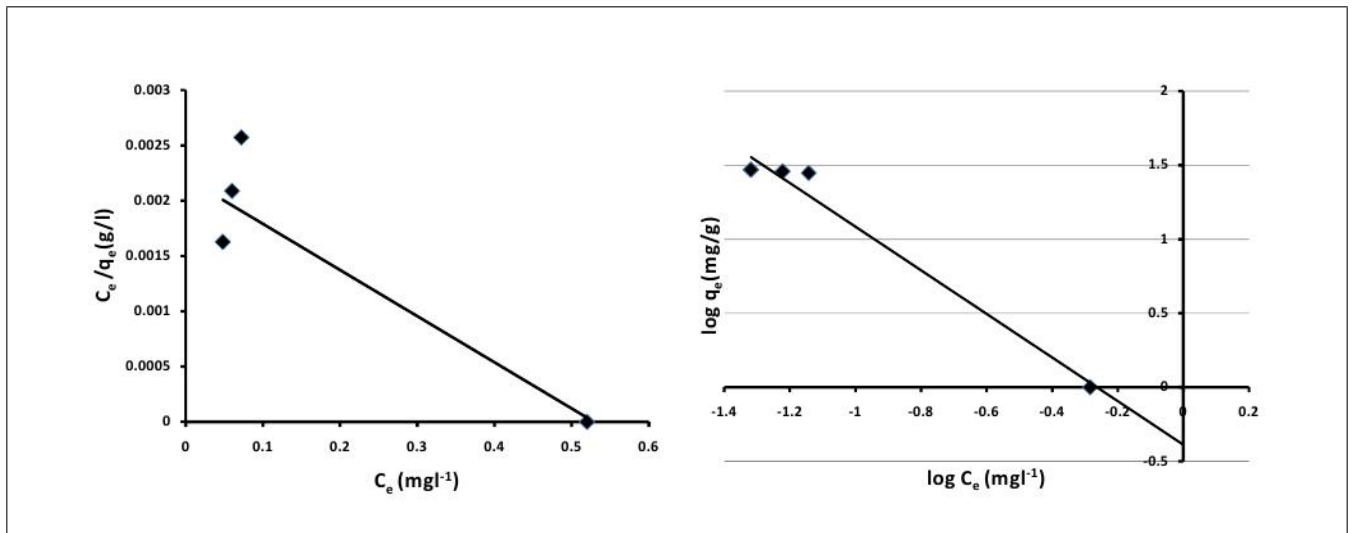


Figure 5.14: (a) Langmuir isotherm model and (b) Freundlich isotherm model of LTA for Ammonia treatment for 60 minutes.

5.6.4 Langmuir and Freundlich Isotherms

Table 5.16 Langmuir parameters for adsorption of Arsenic

Langmuir model			
Adsorbent	q_m (mg ⁻¹)	b (lmg ⁻¹)	R^2
LTX	19.6078	9.8039×10^{03}	0.594
LSX	16.3934	1.6393×10^{04}	0.954
LTA	14.0845	1.4084×10^{04}	0.936

Table 5.17 Freundlich parameters for adsorption of Arsenic

Freundlich model				
Adsorbent	$1/n$	K ((mgg ⁻¹)(mg ^l ⁻¹) ⁿ)	R^2	n
LTX	0.601	1.7394	0.508	1.664
LSX	0.274	2.7582	0.771	3.650
LTA	0.073	6.5104	0.361	13.699

Table 5.18 Langmuir parameters for adsorption of Ammonia

Langmuir model			
Treatment time	q_m (mg ⁻¹)	b (lmg ⁻¹)	R^2
30 mins	-500	-250000	0.235
60 mins	-250	-2	0.799

Table 5.19 Freundlich parameters for adsorption of Ammonia

Freundlich model				
Treatment time	1/n	K ((mgg ⁻¹)(mg ^l ⁻¹) ⁿ)	R ²	n
30 mins	-1.220	-0.4248	0.789	-0.82
60 mins	-1.472	1.0563	0.976	-0.6793

5.7 Discussion

5.7.1 Zeolites

SEM micrographs of synthesized zeolites showed that the zeolites had highly crystalline morphology. Average size was between 2 – 10 μm , and which is also similar to results obtained by Kwakye-Awuah (2008) for LTX and LTA. TGA results also confirmed thermal stability of zeolites. Initial loss of weight can be attributed to the loss of water molecules still trapped in the pores and channels of the zeolite frameworks as Concepción et al. (1996) observed. The results also confirmed the thermal stability of the zeolites at temperatures up to 1000 °C. XRD patterns of the synthesized zeolites did not have flat bases in (Khemthong et al., 2007; Kwakye-Awuah, 2008). However, the positions of peaks did match those in these studies. The first peak position of LTX appeared at 6 ° as in previous studies. The positions of the other peaks were confirmed though they had higher intensities. XRD pattern of LTA was also confirmed by Kwakye-Awuah (2008). According Ojha et al. (2004), the two most intense bands of zeolites usually occur at 860–1230 cm^{-1} and 420–500 cm^{-1} this agrees with the FTIR spectrum of synthesized zeolites in this study. The absorbance band in between the wave numbers 980–1320 cm^{-1} in the spectra represents the presence of substituted Al atoms in the tetrahedral forms of the silica frameworks (Ojha et al., 2004). Asymmetric stretching caused by internal vibrations also occurred at 968 cm^{-1} for LTX, 962 cm^{-1} for LSX and 971 cm^{-1} for LTA, due to the overlapping of asymmetric vibrations of Si–O (bridging) and Si–O (non-bridging). T–O bending also occurred at 426 cm^{-1} for LTX, 423 cm^{-1} and 442 cm^{-1} for LTA.

5.7.2 Arsenic Removal

The maximum contaminant level of arsenic in drinking water is 0.01 mg/l (WHO, 2011). According to Shevade et al. (2001), H^+ and NH_4^+ forms of synthetic zeolites were capable of removing of arsenic to less than 0.05 mg/l within 15 minutes, however, the removal time in this study was 30 minutes. This time was chosen after kinetics indicated that the best period of removing arsenic was 30 minutes. Also, high alumina zeolites have shown to have high exchange capacity in arsenic removal (Shevade et al., 2001). This maybe due to a high concentration of terminol Al–OH species in low Si/Al ration zeolites which leads to a greater capacity for a ligand exchange reaction. The sorption data were fitted to the Langmuir and Freundlich equations, the parameters are given in Tables 5.16 and 5.17. For all cases, the Langmuir model represents a better fit to the experimental data than the Freundlich model and this was also observed in Hui et al. (2005) and this agrees with the R^2 obtained in the Freundlich plots. LTX had an equilibrium sorption capacity (q_m) of 19.6078 mgg^{-1} and LSX and LTA had 16.3934 mgg^{-1} and 14.6845 mgg^{-1} respectively. This agrees with the removal efficiencies which makes LTA the best adsorbent since with the lowest q_m , thus, the volume of adsorbate required to form a monolayer on the adsorbent (LTA) was less than that of LTX and LSX. This confirms the relationship that the maximum adsorption capacity of an adsorbent is inversely proportional to its slope. Thus, the lower the slope or gradient of adsorption, the higher the adsorption capacity. This also confirms the relationship as in equation 4.11, thus, the energy required to bind the adsorbate to the adsorbent is proportional to the slope, hence, a higher slope implies a higher gradient of adsorption which will require a higher energy of adsorption b and this is reflected in Table 5.16. The Freundlich isotherm, however, indicates that LTA had a very high adsorption capacity due to its low intercept and slope, thus confirming the relationship between adsorption capacity and gradient of adsorption. The adsorption intensity ($1/n$) gives an indication of the favourability of the adsorption. The high n values of LTA indicate a high favourability of adsorption by LTA. According to Shevade and Ford (2004), arsenic concentration decreased as a function of time, this was not confirmed in this study as results kinetics (Table 5.2). This could be due to the adsorbent's (LTX) low removal efficiency of arsenic.

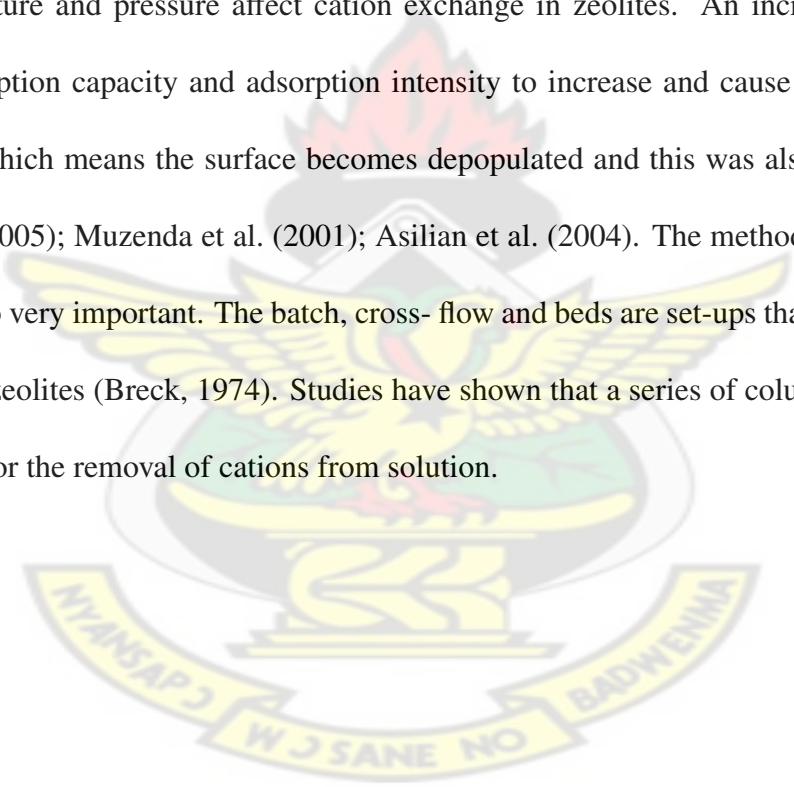
5.7.3 Ammonia Removal

Adsorption isotherms for the adsorbents were fitted to the Langmuir (as in Lahav and Green (1998)) and Freundlich equations. Previous studies of ammonia removal obtained efficiencies of 93 to 98 % (Rahmani and Mahvi, 2006) while removal efficiencies for this study were 76.67 to 93.33 % and 86.15 to 90.77 % for treatment times of 30 and 60 minutes respectively. R^2 values obtained for the Freundlich isotherm gives a good correlation co-efficient value as compared to the values obtained from the Langmuir isotherm and this was also compared with results obtained in Lahav and Green (1998). In Rahmani and Mahvi (2006), it was observed that other ions competed with ammonia and it is possible this also occurred in this study though was not a measured parameter. LTA was the only adsorbent used for ammonia removal. The maximum adsorption capacity (q_m) obtained with corresponding energy of adsorption recorded was very lower for treatment for 30 minutes as compared with that of treatment for 60 minutes (Table 5.18). This can be attributed to the negative slope which is related to the maximum adsorption capacity and energy of adsorption (equations 4.10, 4.11). From the Freundlich isotherm, the adsorption capacity and intensity of treatment after 60 minutes was better than that of treatment for 30 minutes as shown in Table 5.19. The negative slope accounts for the leaching of ammonia back into the solution from the zeolite framework as time increases.

5.7.4 Other Variables Affecting Cation Exchange in Zeolites

The pH of the aqueous solution is an important controlling parameter in the sorption process (Hui et al., 2005). Removal efficiency will either increase or decrease with change in pH. The selectivity of ions by zeolites is also influenced by the character of the ion that predominates at a particular solution pH. Exposure of the zeolite surface to water causes the ionization of the surface hydroxyl groups (Si-OH and Al-OH). The degree of ionisation depends on pH, and the acid/base reaction occurring at the hydroxyl groups may result in surface charge development. Zeolites are also capable of affecting solution pH due to their higher internal pH. The zeolite surface may be influenced by the ambient pH which is not equal to the external solution pH value and precipitation within the channels and surface of zeolites may occur (Hui et al., 2005). The types and concentration of anions, competing cations and complex agents

can each alter the quality of ion exchange separation which can be achieved. Due to the rigidity of the zeolite framework however, the effects of these variables are minimal. Metal sorption by synthetic zeolites decreased with decreasing pH. This trend was observed in this study though not an objective of the study. This can be attributed to the influence of zeolites on solution acidity, tending to neutralize the solution by exchange of H^+ with the cations initially present in their structures (Álvarez-Ayuso et al., 2003; Shevade and Ford, 2004; Hui et al., 2005). The competitive exchange of H^+ is considered to be the reason of lower retention of metals in more acidic environment (Álvarez-Ayuso et al., 2003; Shevade and Ford, 2004). The pH also has a significant effect on ammonia removal since it affects both ion chemical speciation and zeolites (Zabochnicka-Swiątek and Malńska, 2010) From the results obtained above, temperature and pressure affect cation exchange in zeolites. An increase in temperature will cause the adsorption capacity and adsorption intensity to increase and cause a decrease in the energy of adsorption which means the surface becomes depopulated and this was also observed in Payne and Abdel-Fattah (2005); Muzenda et al. (2001); Asilian et al. (2004). The method used to study the cation exchange is also very important. The batch, cross- flow and beds are set-ups that have been implemented in the study of zeolites (Breck, 1974). Studies have shown that a series of columns containing zeolite is most effective for the removal of cations from solution.



CHAPTER 6

CONCLUSION AND SUGGESTIONS FOR FUTURE WORK

6.1 Conclusion

The removal of Arsenic and Ammonia wastewater samples was successful. Their levels after treatment was below the maximum contaminant level set by the Ghana EPA. Based on this experimental study, the following conclusions can be made:

1. Synthesis of zeolites were successful and characterizations confirmed this.
2. The maximum contaminant level of the WHO can be attained upon repeating treatment of samples.
3. The removal efficiencies ranged between 67.86–81.35 % for LTX, 67.86–86.31 % for LSX and 71.87–96.00 % for LTA
4. The adsorbent LTA had the best removal efficiency followed by LSX and LTX. After this time, leaching of ammonia back into the solution begins.
5. The removal efficiencies ranged between 76.67–93.33 % and 86.15–90.77 % for treatment for 30 minutes (sample 1) and 60 minutes (sample 2).
6. The Langmuir parameters, maximum adsorption capacity (q_m) and energy of adsorption (b) were dependent on the slope or gradient of adsorption.
7. The Freundlich parameters, adsorption capacity (K) and adsorption intensity ($1/n$) were also dependent on the slope or gradient of adsorption.

8. The Langmuir isotherm of LTX for arsenic removal obtained was $q_e = 19.6078 \times 9.8039 \times 10^3 C_e / 1 + 9.8039 \times 10^3 C_e$ with an R^2 of 0.594. The Freundlich isotherm obtained was $\log q_e = \log 1.7394 + 0.601 \log C_e$ with an R^2 of 0.508.
9. The Langmuir isotherm of LSX for arsenic removal obtained was $q_e = 16.3934 \times 1.6393 \times 10^4 C_e / 1 + 1.6393 \times 10^4 C_e$ with an R^2 of 0.954. The Freundlich isotherm obtained was $\log q_e = \log 2.7582 + 0.274 \log C_e$ with an R^2 of 0.771.
10. The Langmuir isotherm of LTA for arsenic removal obtained was $q_e = 14.0845 \times 1.4084 \times 10^4 C_e / 1 + 1.4084 \times 10^4 C_e$ with an R^2 of 0.936. The Freundlich isotherm obtained was $\log q_e = \log 6.5104 + 0.073 \log C_e$ with an R^2 of 0.361.
11. The Langmuir isotherm of LTA for ammonia removal after 30 minutes of treatment was $q_e = -500 \times -2.5 \times 10^5 C_e / 1 + -2.5 \times 10^5 C_e$ with an R^2 of 0.936. The Freundlich isotherm obtained was $\log q_e = \log -0.4248 - 1.220 \log C_e$ with an R^2 of 0.789.
12. The Langmuir isotherm of LTA for ammonia removal after 60 minutes of treatment was $q_e = -250 \times -2 C_e / 1 + -2 C_e$ with an R^2 of 0.936. The Freundlich isotherm obtained was $\log q_e = \log 1.0563 - 1.472 \log C_e$ with an R^2 of 0.976.

6.2 Suggestions for future work

Due to time and financial constraints, the scope of this work was limited. However, based on the present study, some recommendations can be made;

Firstly, the use of alternative materials such as bauxite, rice husk, clay and plantain peels should be encouraged to reduce cost of reagents.

Secondly, ion exchange occurred at room temperature. The effect of temperature changes should be investigated as this will contribute to a greater understanding of the adsorption process.

Thirdly, zeolites used should be regenerated using NaCl and the brine obtained can be used for agricultural purposes and the zeolites used again. Fourthly, treatment of samples should be repeated

with either fresh zeolites or regenerated zeolites as this has the ability to remove the contaminants to negligible levels or even to 0.

Finally, the use of alternate methods such as columns or beds is highly recommended.

KNUST



Bibliography

1. Álvarez-Ayuso, E., García-Sánchez, A., and Querol, X. (2003). Purification of metal electroplating waste waters using zeolites. *Water Research*, 37:4855–4862.
2. Asilian, H., Mortazavi, S. B., Kazemian, H., Phaghieh-zadeh, S., Shahtaheri, S. J., and Salem, M. (2004). Removal of ammonia from air using three Iranian natural zeolites. *Iranian J. Publ Health*, 33(1):45–51.
3. Baerlocher, C., McCusker, L., and Olson, D. H. (2007). *Atlas of zeolite framework types*. Elsevier, Amsterdam, 6th revised edition.
4. Barrer, R. M. (1945). Separation of mixtures using zeolites as molecular sieves. i. three classes of molecular-sieve zeolite. *J. Soc. Chem. Ind.*, 64:130.
5. Barrer, R. M. (1948a). Sorptive and molecular sieve properties of a new zeolitic mineral. *J. Soc. Chem. Ind.*, page 133.
6. Barrer, R. M. (1948b). Synthesis and reactions of mordenite. *J. Soc. Chem. Ind.*, page 2158.
7. Barrer, R. M. (1948c). Synthesis of a zeolitic mineral with chabazite-like sorptive properties. *J. Soc. Chem. Ind.*, page 127.
8. Barrer, R. M. (1979). Chemical nomenclature and formulation of compositions of synthetic and natural zeolites. *Pure and Applied Chemistry*, 51(5):1091–1100.
9. Barrer, R. M. (1982). *Hydrothermal chemistry of zeolites*. Academic Press, New York.

10. Barthomeuf, D. (1996). Basic zeolites: Characterisation and uses in adsorption and catalysis. *Catalysis Reviews*, 38(4):521–612.
11. Bedard, R. L., Bein, T., Davis, M. E., Garcia, J., Maroni, V. A., and Stucky, G. D., editors (1991). *Nanoscale engineered ceramics from zeolites: creating the ideal precursor for high-quality cordierite, in synthesis/characterization and Novel Applications of molecular sieve materials*, volume 233.
12. Bell, R. G. (2001). What are zeolites.
13. Blöcher, C., Dorda, J., Mavrov, V., Chmiel, H., Lazaridis, N. K., and Matis, K. A. (2003). Hybrid floatation - membrane filtration process for the removal of heavy metal ions from wastewater. *Water Research*, 37:4018–4026.
14. Breck, D. W. (1974). *Zeolite molecular sieves, structure, chemistry and use*. John Wiley & Sons, Inc., New York.
15. Casado, L., Mallada, R., Téllez, C., Coronas, J., Menéndez, M., and Santamaría, J. (2003). Preparation, characterisation and pervaporation performance of mordenite membranes. *Journal of Membrane Science*, 216:135–147.
16. Concepción, P., López Nieto, J. M., Mifsud, A., and Perez-Pariente, J. (1996). Preparation and characterization of mg-containing afl and chabazite-type materials. *Zeolites*, 16:56–64.
17. Coronas, J. and Santamaria, J. (2004). The use of zeolite films in small-scale and micro-scale applications. *Chemical Engineering Science*, 59:4879–4885.
18. Cundy, C. S. and Cox, P. A. (2005). the hydrothermal synthesis of zeolites: Precursors, intermediates and reaction mechanism. *Microporous and Mesoporous Materials*, 82:1–78.
19. Currao, A. Understanding zeolite frameworks.
20. Dąbrowski, A., Hubicki, Z., Podkościelny, P., and Robens, E. (2004). Selective removal of the heavy metal ions from waters and industrial wastewaters by ion-exchange method. *Chemosphere*, 56:91–106.

21. Duarte, A. A. L. S., Cardoso, S. J. A., Alçada, A. J., et al. (2009). Emerging and innovative techniques for arsenic removal applied to a small water supply system. *Sustainability*, 1:1288–1304.
22. Dyer, A. and Zubair, M. (1998). Ion-exchange in chabazite. *Microporous and Mesoporous Materials*, 22:135–150.
23. Eisazadeh, H. (2008). Removal of arsenic in water using polypyrrole and its composites. *World Applied Sciences*, 3(1):10–13.
24. Ertl, G., Knözinger, H., and Weitkamp, J. (1999). *Preparation of solid catalysts*. WILEY-VCH Verlag GmbH, Weinheim.
25. Hui, K. S., Chao, C. Y. H., and Kot, S. C. (2005). Removal of mixed heavy metal ions in wastewater by zeolite 4a and residual products from recycled coal fly ash. *Journal of Hazardous Materials*, B127:89–101.
26. Karger, J. and Ruthven, D. M. (1992). *Diffusion in zeolites and other microporous solids*. John Wiley & Sons, Inc.
27. Khemthong, P., Prayoonpokarach, S., and Wittayakun, J. (2007). Synthesis and characterization of zeolite lxx from rice husk silica. *Suranaree J. Sci. Technol.*, 14(4):367–379.
28. Köhl, G. H. (1987). Crystallization of low-silica faujasite. *Zeolites*, 7:451–457.
29. Kulprathipanja, S., editor (2010). *Zeolites in Industrial Separation and Catalysis*. WILEY-VCH Verlag GmbH & Co. KGaA.
30. Kwakye-Awuah, B. (2008). *Production of silver-loaded zeolites and investigation of their antimicrobial activity*. PhD thesis, University of Wolverhampton.
31. Kwakye-Awuah, B., Radecka, I., Kenward, M. A., and Williams, C. D. (2008). Production of silver-doped analcime by isomorphous substitution technique. *Journal of Chemical Technology and Biotechnology*, 83:1255–1260.

32. Lahav, O. and Green, M. (1998). Ammonium removal using ion exchange and biological regeneration. *Water Research*, 32(7):2019–2028.
33. Lazaridis, N. K., Zouboulis, A. I., Gallios, G. P., and Mavrov, V. (2005). A hybrid flotation - microfiltration process for metal ions recovery. *Journal of Membrane Science*, 247:29–35.
34. Lechert, H. and Kacirek, H. (1991). Investigations on crystallization of x-type zeolites. *Zeolites*, 11:720–728.
35. Lechert, H. and Kacirek, H. (1993). Kinetics of nucleation of x zeolites. *Zeolites*, 13.
36. Leonard, R. J. (1927). The hydrothermal alteration of certain silicate minerals. *Econ. Geol.*, 22:18–43.
37. Matis, K. A., Zouboulis, A. I., Gallios, G. P., Erwe, T., and Blöcher, C. (2004). Application of flotation for the separation of metal-loaded zeolites. *Chemosphere*, 55:65–72.
38. Matis, K. A., Zouboulis, A. I., and Lazaridis, N. K. (1998). *Removal and recovery of metals from dilute solutions applications of floatation techniques*. Kluwer Academic Publ., Netherlands.
39. McBain, J. W. (1932). *The sorption of gases and vapours by solids*. Rutledge and Sons, London.
40. McCusker, L., Liebau, F., and Engelhardt, G. (2003). Nomenclature of structural and compositional characteristics of ordered microporous and mesoporous materials with inorganic hosts (iupac recommendations 2001). *Microporous and Mesoporous Materials*, 58(11):3–13.
41. Meier, W. M. and Olson, D. H. (1988). *Atlas of zeolite structure types*. Butterworth & Co. Ltd., University Press, Cambridge, UK, 2nd revised edition.
42. Mercer, B. W., Ames, L. L., Touhill, C. J., Slyke, W. J. V., and Dean, R. B. (1970). Ammonia removal from secondary effluents by selective ion exchange. *Water Pollution Control Federation*, 42(2):R95–R107.
43. Meteš, A., Kovačević, D., Vujević, D., and Papić, S. (2004). The role of zeolites in wastewater treatment of printing inks. *Water Research*, 38:3373–3381.

44. Milton, R. M. (1989). Molecular sieve and technology: a historical perspective, in zeolite synthesis. *ACS Symposium Series*, 398:1–10.
45. Muzenda, E., Kabuba, J., Ntuli, F., and Mollagee, M. (2001). Kinetics study of ammonia removal from synthetic waste water. *World Academy of Science, Engineering and Technology*, 79.
46. Nguyen, M. L. and Tanner, C. C. (1998). Ammonium removal from wastewaters using natural new zealand zeolites. *New Zealand Journal of Agricultural Research*, 41:427–446.
47. Occelli, M. L. and Kessler, H., editors (1997). *Synthesis of porous materials: Zeolites, clays and nanostructures*.
48. Ojha, K., Pradhan, N. C., and Samanta, A. N. (2004). Zeolite from fly ash: synthesis and characterization. *Bull. Mater. Sci.*, 27(6):555–564.
49. Ozin, G. A., Kuperman, A., and Stein, A. (1989). Advanced zeolite material science. *Angew. Chem. Int. Ed.*, 28:359–376.
50. Pauling, L. (1930a). The structure of sodalite and helvite. *Z. Kristallogr.*, 74:213.
51. Pauling, L. (1930b). The structure of some sodium and calcium aluminosilicates. *Proc. Natl. Acad. USA*, 16:453.
52. Payne, K. B. and Abdel-Fattah, T. M. (2005). Adsorption of arsenate and arsenite by iron-treated activated carbon and zeolites: Effects of pH, temperature and ionic strength. *Journal of Environmental Science and Health*, 40:723–749.
53. Pingxiang Naike Chemical Industry Equipment Packing Co., L. Difference between molecular sieves and zeolites.
54. Pontius, F. W. (1994). Crafting a new arsenic rule. *Journal of American Water Works Association*, 86(9).
55. Rahmani, A. R. and Mahvi, A. H. (2006). Use of ion exchange for removal of ammonium: A biological regeneration of zeolite. *Globalnest Journal*, 8(2):146–150.

56. Rahmani, A. R., Mahvi, A. H., Mesdaghinia, A. R., and Nasser, S. (2004). Investigation of ammonia removal from polluted waters by clinoptilolite zeolite. *International Journal of Environmental Science and Technology*, 1(2):125–133.
57. Rouquerol, J. et al. (1994). Recommendations for the characterisation of porous solids. Technical Report 8, IUPAC.
58. Shevade, S., Ford, R., and Puls, R. (2001). Arsenic separation from water using zeolites. *Am Chem Soc Div Environ Res*, 41(2):Part 1.
59. Shevade, S. and Ford, R. G. (2004). Use of synthetic zeolites for arsenate removal from pollutant water. *Water Research*, 38:3197–3204.
60. Sobolev, V. I., Panov, G. I., Kharitonov, A. S., Romanikov, V. N., Volodin, V. N., and Ione, K. G. (1993). Catalytic properties of zsm-5 zeolites in n_2o decomposition: the role of iron. *Journal of Catalysis*, 139(2):435–443.
61. Szostak, R. (1989). *Molecular sieves, science and technology*. Springer, Berlin.
62. Taylor, W. H. (1930). The crystal structure of analcite ($naalsi_2o_6.h_2o$). *Z. Kristallogr.*, 74:1.
63. the free encyclopedia Wikipedia (2012). Wikipedia; the free encyclopedia.
64. Thompson, R. W. (1998). *Molecular sieves, science and technology*. Springer, Berlin.
65. Thompson, R. W. and Huber, J. M. (1982). Analysis of the growth of molecular sieve zeolite NaA in a batch precipitation system. *Journal of Crystal Growth*, 56:711–722.
66. Townsend, R. P. (1986). Ion exchange in zeolites: some recent developments in theory and practice. *Pure and Applied Chemistry*, 58(10):1359–1366.
67. U.S.E.P.A (1983). *In Methods for Chemical Analysis of Water and Wastes*. United States Environmental Protection Agency, epa-600/4-79-020 edition.

68. Von-Kiti, E. (2011). Synthesis of zeolites and their application to the desalination of seawater. Master's thesis, Kwame Nkrumah University of Science and Technology, Kumasi, Ghana.
69. Vu, K. B., Kaminskiand, M. D., and Nuñez, L. (2003). Review of arsenic removal technologies for contaminated groundwaters. Technical report, Argonne National Laboratory.
70. Wang, Z., Mitra, A., Wang, H., Huang, L., and Yan, Y. (2001a). Pure-silica zeolite low-k dielectric thin films. *Adv. Mater.*, 13:746.
71. Wang, Z., Mitra, A., Wang, H., Huang, L., and Yan, Y. (2001b). Pure-silica zeolite thin films as low-k dielectric thin films. *Adv. Mater.*, 13:1463.
72. Weigel, O. and Steinhoff, E. (1925). Adsorption of organic liquid vapors by chabazite. *Z. Kristallogr.*, 61:125–154.
73. WHO (1996). Ammonia in drinking water.
74. WHO (2011). *Guidelines for drinking water quality*. WHO Press, World Health Organization, 4th edition.
75. Yeom, Y. H. and Kim, Y. (1997). Crystal structure of zeolite x exchanges with pb(ii) at ph 6.0 and dehydrated: $(pb^{4+})_14(pb^{2+})_18(pb_4O_4)_8si_100al_92O_384$. *Journal of Physical Chemistry*, 101(27):5314–5318.
76. Zabochnicka-Swiątek, M. and Malńska, K. (2010). Removal of ammonia by clinoptilolite. *Globalnest Journal*, 12(3):256–261.
77. Zeng, L. (2004). Arsenic adsorption from aqueous solutions on an fe(iii)-si binary oxide adsorbent. *Water Qual. Res. J. Canada*, 39(3):267–275.
78. Zorpas, A. A., Constantinides, T., Vlyssides, A. G., Haralambous, I., and Loizidou, M. (2000). Heavy metal uptake by natural zeolite and metals partitioning in sewage sludge compost. *Bioresource Technology*, 72:113–119.

Appendix A

A.0.1 Calculation to produce 0.01N NaOH

0.01N = M

$$C = \frac{m}{M \times V} \quad (\text{A.1})$$

where:

m = mass

M = molar mass

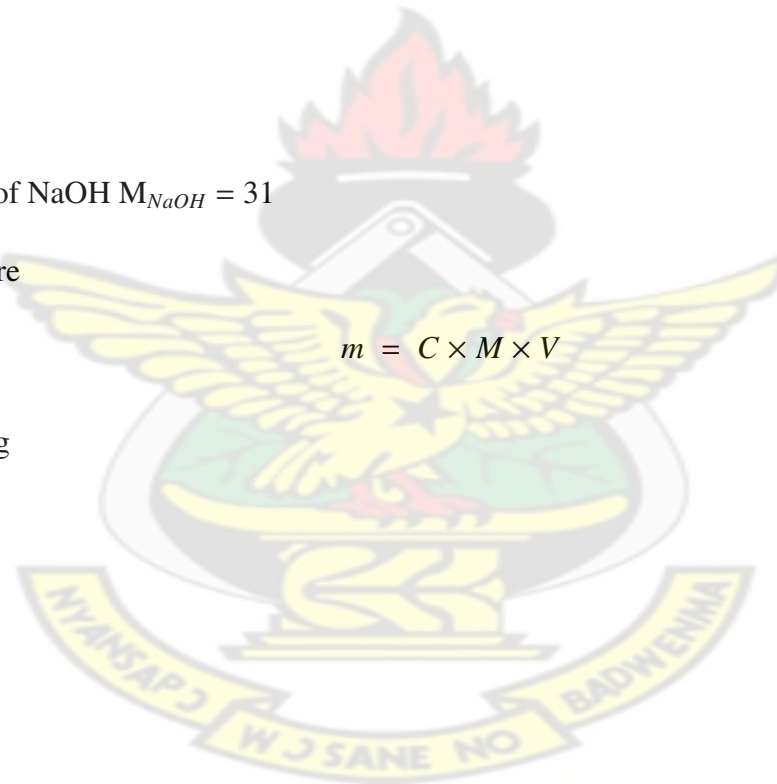
V = volume

Thus for 0.01N of NaOH $M_{\text{NaOH}} = 31$

V = 0.6l therefore

$$m = C \times M \times V \quad (\text{A.2})$$

$\therefore m_{\text{NaOH}} = 18.6\text{g}$



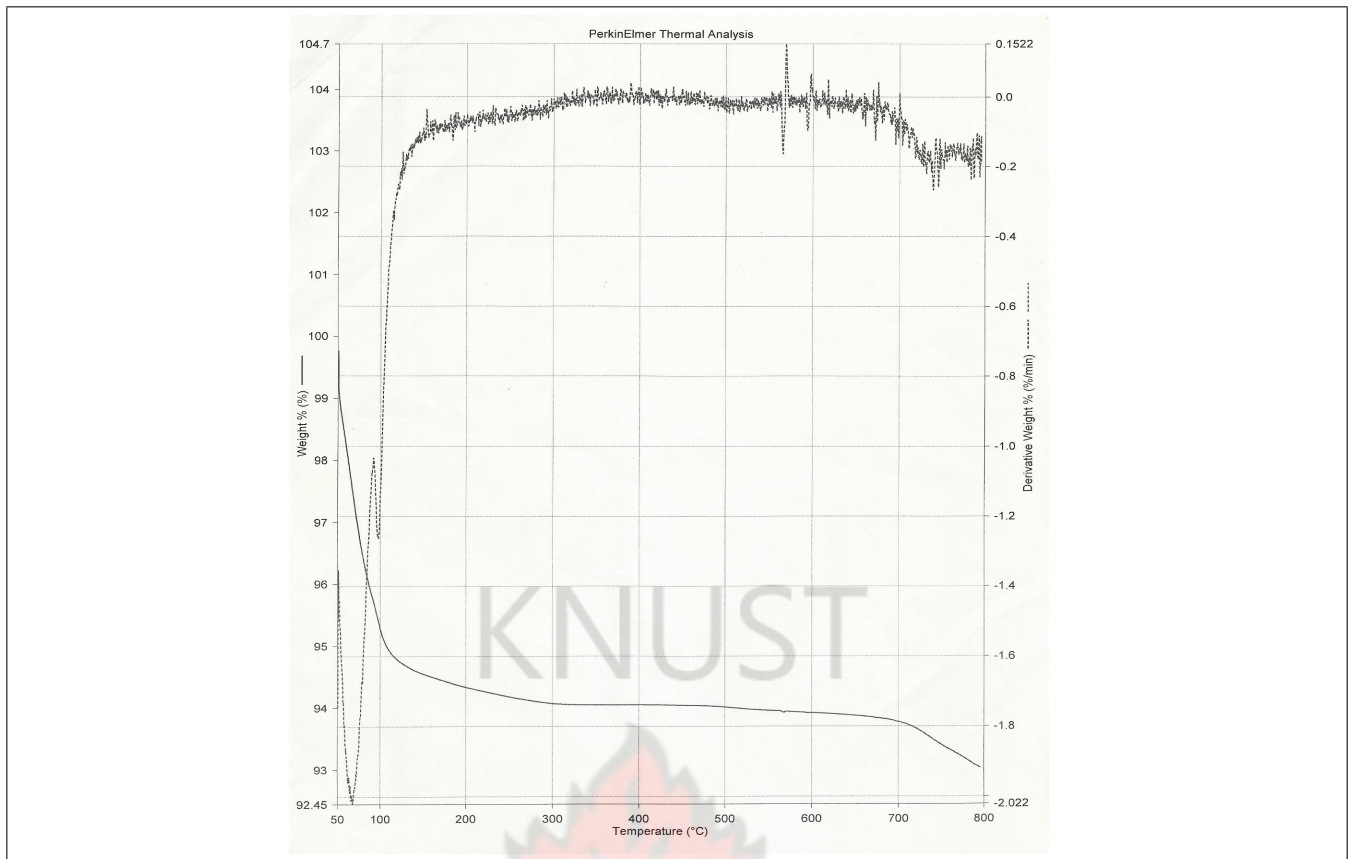


Figure A.1: Thermogravimetric Analysis of LTX

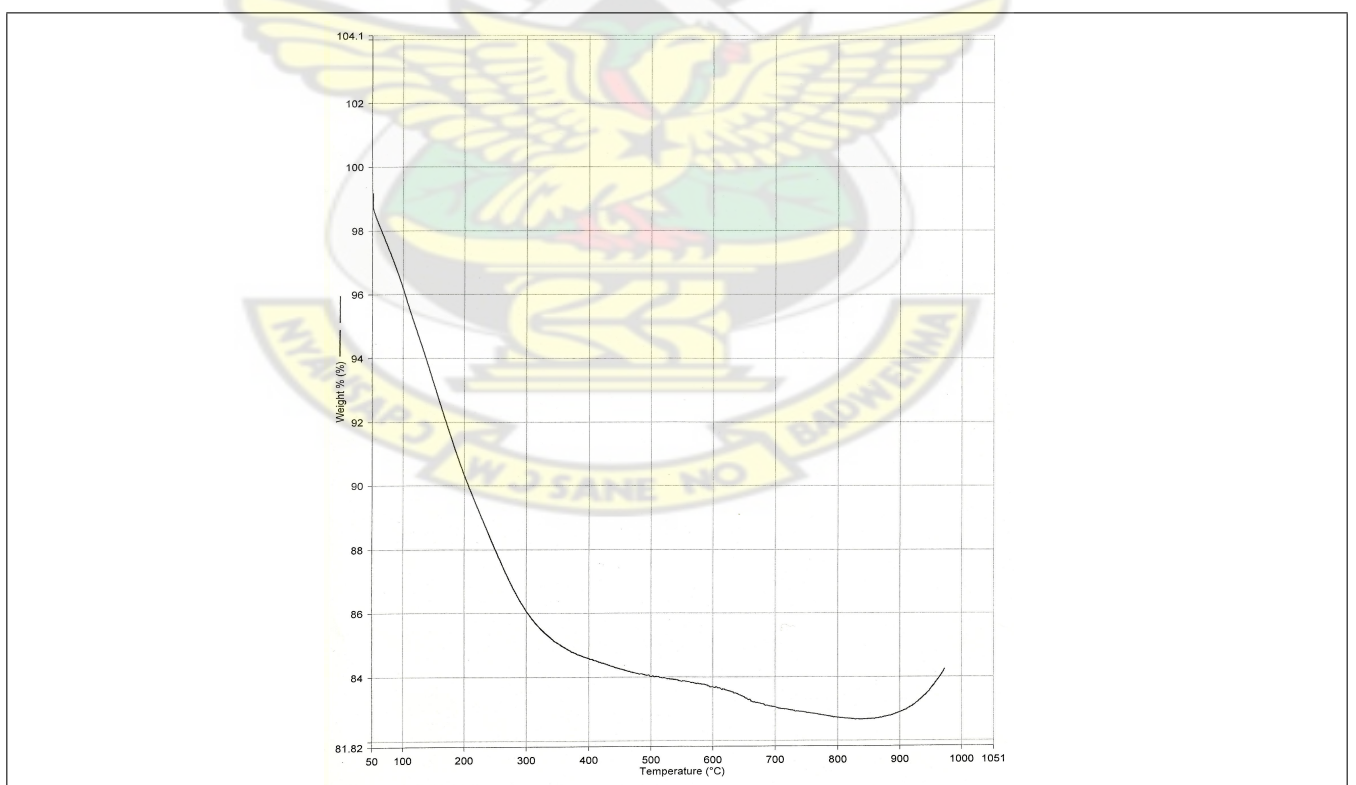


Figure A.2: Thermogravimetric analysis of LSX

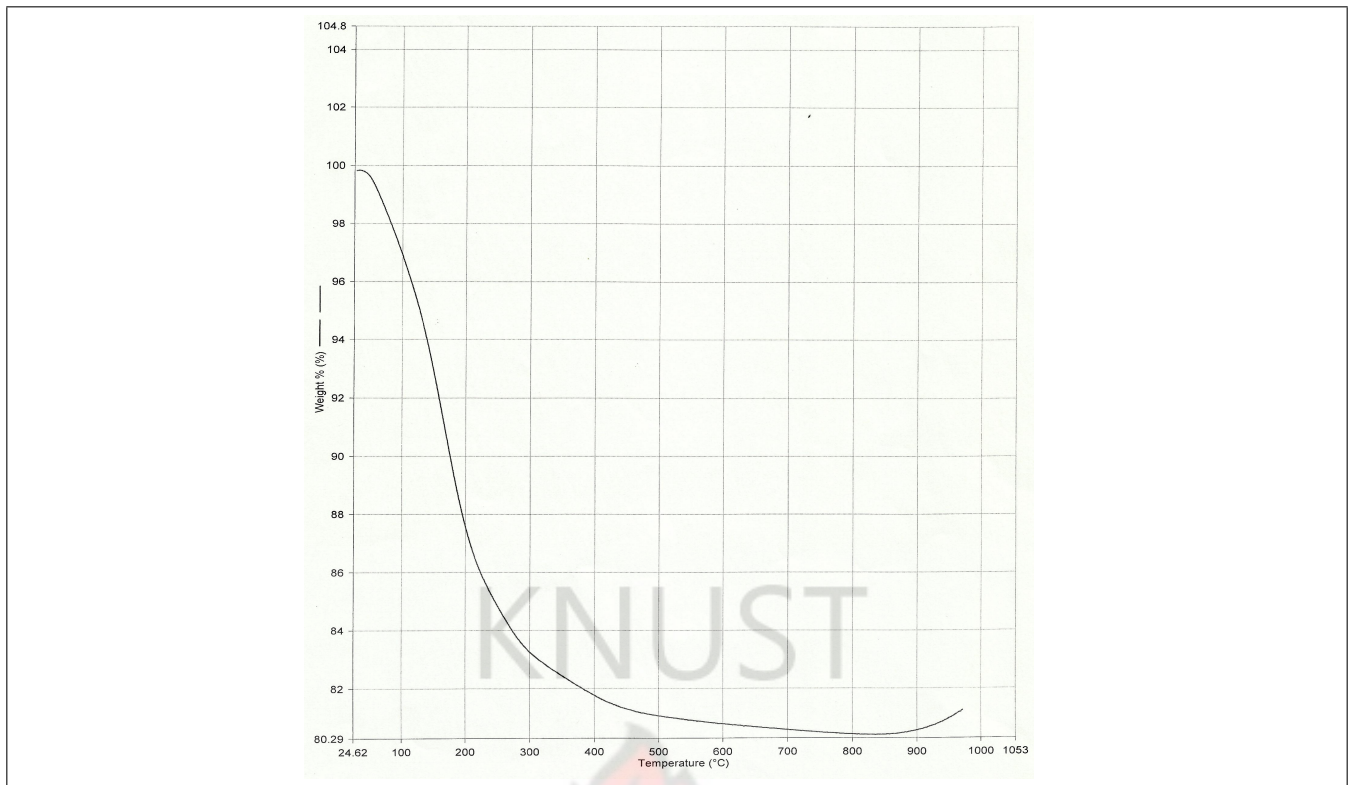


Figure A.3: Thermogravimetric Analysis of LTA

SGS ANALYTICAL REPORT E004897 R0

Sample Number	E004897.001	E004897.002	E004897.003	E004897.004	E004897.005
Sample Name	NYAM 1	NYAM 2	NLTX 30	NLTX 60	NLTX 90
Parameter	Units	LOR			
Hydride T Method: APHA 3114 B, Total					
As (Total)*	mg/L	0.002	-	0.19	0.028
				0.044	0.014
AN300 Method: APHA Method 3110					
Co (Total)*	mg/L	0.03	0.03	-0.03	0.16
				0.09	0.04

Sample Number	E004897.006	E004897.007	E004897.008
Sample Name	NLTX 30	NLTX 60	NLTX 90
Parameter	Units	LOR	
Hydride T Method: APHA 3114 B, Total			
As (Total)*	mg/L	0.002	0.042
			0.076
			0.000
AN300 Method: APHA Method 3110			
Co (Total)*	mg/L	0.03	0.18
			0.23
			0.26

Figure A.4: Results of ICP-OES from SGS Lab of Kinetics

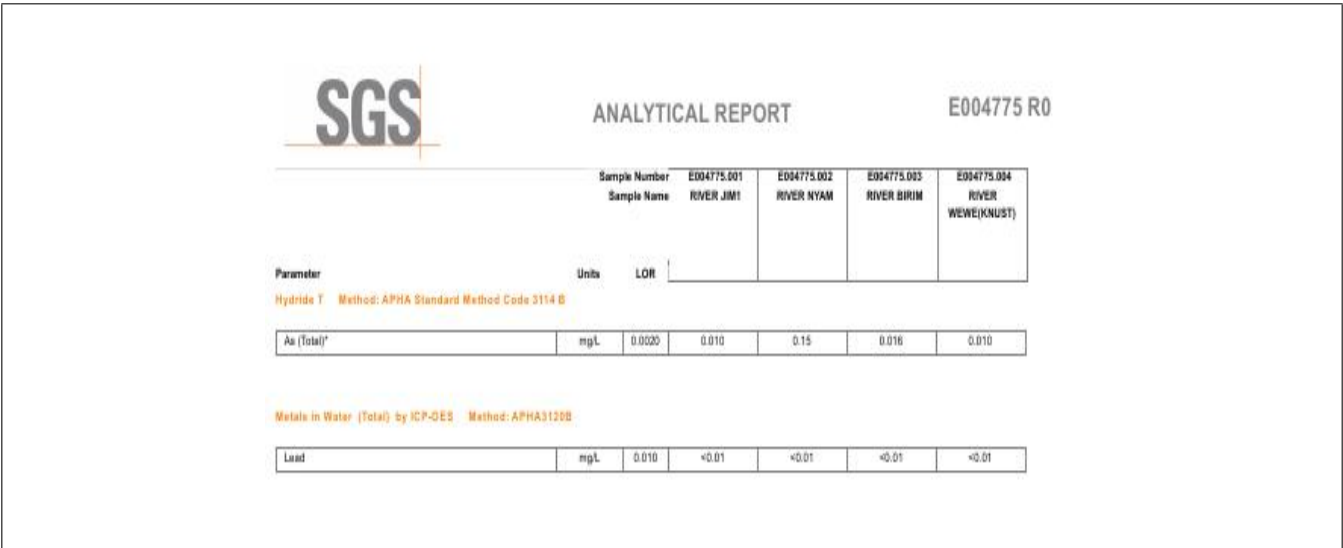


Figure A.5: Results of ICP-OES from SGS Lab of other Sample sites



Appendix B

B.1 Used Softwares

- \LaTeX : typesetting and layout
- GNU Image Manipulation Program (GIMP) : graphics
- Microsoft Excel : data processing
- Matlab : Data processing and graphs
- CorelDrawX5 : graphics

